Does Frequent Low Resolution Feedback Outperform Infrequent High Resolution Feedback for Multiple Antenna Beamforming Systems?

Taejoon Kim, *Student Member, IEEE*, David J. Love, *Senior Member, IEEE*, and Bruno Clerckx, *Member, IEEE*

***Abstract*—Multiple antenna systems that adapt to the channel conditions are known to provide numerous rate and reliability benefits. In frequency division duplexing, the transmitter typically learns about the channel conditions using a small amount of feedback (called limited feedback) sent on the reverse link. While feedback is well studied, there has been only limited work addressing how feedback techniques should be modified depending on the amount of mobility. This paper concerns a signaling scheme for limited feedback multiple antenna wireless communications taking the temporal correlation into account during feedback design. We refer to this as using an adaptive feedback period (AFP) scheme. In the AFP scheme, the transmitter and receiver reuse the past channel state information (CSI) as side information. Feedback to be used for several channel uses is sent from the receiver to the transmitter using a predetermined feedback update period. The feedback update period is determined by characterizing the temporal correlation statistic, so that the proposed AFP scheme outperforms the traditional limited feedback approach, which we refer to as the minimal feedback period (MFP) scheme. To measure the performance, the average effective SNR is considered. Bounds on the feedback update period, correlation coefficient, and feedback rate needed for the AFP scheme to outperform the MFP scheme are derived. Moreover, criteria to initiate the control of the feedback update period are obtained. Results on the average effective SNR are used to develop bounds on the feedback update period using the capacity loss. It is also shown that in the large system limit the feedback update periods required for both the average effective SNR and capacity loss converge to the same bound. These results verify that infrequent high resolution feedback is sometimes preferable to frequent low resolution feedback.**

***Index Terms*—Adaptive feedback rate, adaptive feedback update period, multiple-input single-output (MISO) channel, quantized beamforming, temporally correlated channel.**

I. Introduction

As next generation multiple antenna standards evolve, closed-loop systems that adapt the transmitted signal to channel state information (CSI) are growing in popularity because of their many benefits [1]. Because most cellular systems employ frequency division duplexing, CSI is often practically and efficiently obtained from the remote receiver through a digital or analog feedback link. Arguably the most practical approach to conveying this feedback is to use quantized (or limited) feedback. Recently, limited feedback multiple antenna systems have evolved into a key technique for next generation and beyond (i.e., 4 G and beyond) broadband wireless standards (e.g., see the references in [1]).

When the partial CSI is delivered to the transmitter through a finite rate feedback link, transmission schemes that utilize limited feedback as side information show improved performance. Feedback design for beamforming systems is the main focus of [2]–[6]. Optimally quantized directional information of the channel is conveyed to the transmitter, and the works in [3]–[6] verify that the performance benefit arising from quantized channel direction feedback is significant. In these works, codebooks are designed based on independent block fading channel statistics, where the channel varies independently across the temporal blocks.

Although the independent block fading model facilitates the analysis and design of CSI feedback, it neglects to take into account the substantial temporal correlation that is usually present between samples of the multiple-input and multiple-output (MIMO) channel random process. There are several different feedback approaches [7]–[15] accommodating temporal correlation during feedback design. In [7], a single bit of sign feedback is employed to choose a direction of the stochastic perturbation which provides an estimate for the gradient vector to track the dominant channel subspaces. This stochastic perturbation idea and insight from geodesic interpolation in the Grassmannian manifold are extended in [8] where the improvement of the tracking performance is achieved by modeling the trajectory of the channel subspace variation as a geodesic on the Grassmannian manifold. The idea of geodesic modeling on the Grassmannian manifold is extended to a geodesic prediction algorithm in [9]. The channel subspace tracking problem is investigated in the context of successive codebook adaptations [10]–[14]. Flexible codebook switching approaches, where the codebook is switched in a supercodeset in order to track the observed channel variations, are proposed in [10]. Similarly, a spherical cap codebook switching algorithm using a codebook chosen in a supercodeset is considered in [11]. Based on a probabilistic model of the feedback state transition, a local codebook transition approach is proposed in [12] and [13]. Note that [12] and [13] require less feedback overhead than [10], [11] because the codebook switching follows a predefined algorithm based on the state transition statistics, while [10] and [11]

Manuscript received March 23, 2010; revised August 22, 2010; accepted November 12, 2010. Date of publication December 13, 2010; date of current version March 09, 2011. The associate editor coordinating the review of this manuscript and approving it for publication was Prof. Erik G. Larsson. This work was supported in part by Samsung Electronics. The material in this paper was presented at the IEEE International Conference on Acoustics, Speech, and Signal Processing, March 2010, and the IEEE Global Communications Conference, Miami, FL, December 2010.

T. Kim and D. J. Love are with the School of Electrical and Computer Engineering, Purdue University, West Lafayette, IN, 47907 USA (e-mail: kim487@ecn.purdue.edu; djlove@ecn.purdue.edu).

B. Clerckx is with the DMC R&D Center, Samsung Electronics, Yongin-Si, Gyeonggi-Do, 446-712 Korea (e-mail: bruno.clerckx@samsung.com).

Color versions of one or more of the figures in this paper are available online at http://ieeexplore.ieee.org.

Digital Object Identifier 10.1109/TSP.2010.2099222

need additional feedback to notify the index of the codebook whenever switching is required. Differential feedback, where the amount of the perturbation added to the previous precoder is determined by the statistics of the directional variation, is also considered in [14]. In [15], quantized CSI is modeled by a feedback-state Markov chain and the information rate of the CSI quantizer and effect of feedback delay are analyzed.

The time correlated channel can be effectively modeled as a first-order Gauss-Markov process that describes the current channel realization as dependent on the previous channel realizations, which more closely models the real channel. By employing a first-order Gauss-Markov process, conditions on the input distribution achieving capacity in a temporally correlated fading channel are studied in [16]. Using a first-order Gauss-Markov fading model and the assumption of no instantaneous CSI at the transmitter, it is shown in [17] that multiple antenna systems utilizing correlation statistics to decode the signal outperform systems that do not adapt to the correlation in the high SNR regime. The work in [10], [14] also employ the first-order Gauss-Markov model.

In this work, we integrate temporal correlation into the feedback design and investigate how the feedback update period, feedback rate, and average feedback overhead should scale with temporal correlation in the beamforming systems. We attempt to answer the question, "When using feedback for transmission over a temporally correlated channel, is it better to employ frequent low resolution feedback or infrequent high resolution feedback?" We show that infrequent high resolution feedback sometimes can be preferable to high frequency low resolution feedback. This analysis is performed using random vector quantization codebooks [18] to allow analytical solutions.

In beamforming systems, it is known that the beamformer must be chosen to maximize the effective SNR in order to minimize the average BER and maximize the capacity [19], [20]. For quantized beamforming systems, it is shown that the average capacity distortion can be upper bounded by the average effective SNR distortion [4] implying that average effective SNR can be used to characterize the capacity performance. Thus, following the analysis in [2], [4], [6], and [21], we choose to use the average effective SNR as a performance metric to design the limited feedback system. Given these assumptions, we consider a scheme where the previously fed back beamforming vector is used as side information. This feedback occurs periodically according to some *feedback update period* . Given a performance threshold, a bound on the feedback update period is derived and feedback update control criteria are characterized. To further investigate the influence of the temporal correlation, a bound on the feedback rate (or codebook size) of the feedback update control scheme necessary to ensure a nontrivial update period is derived. In addition, a closed-form expression for the average effective SNR are used to develop approximated bounds on the feedback update period for the capacity loss. To gain intuition about bounds on the feedback update period for two different performance metrics (i.e., effective SNR and capacity), large system limit analysis is also performed.

This paper is organized as follows. In Section II, our system model and problem statement are presented. Section III derives bounds on the feedback update period and bounds on the feedback rate. In Section IV, asymptotic analysis is performed. Simulation results are given in Section V. Section VI provides some concluding remarks.

Notations: * denotes conjugate transposition, a bold lowercase letter $\mathbf{a}$ denotes a vector, a_i denotes the ith element of a vector $\mathbf{a}$, $||\mathbf{a}||$ denote the vector 2-norm, $\log_b(\cdot)$ denotes the logarithm with base b, $\ln(\cdot)$ denotes the natural logarithm, and $\Gamma(\cdot)$ denotes the gamma function.

II. System Overview and Problem Formulation

A limited feedback multiple-input single-output (MISO) beamforming system where the transmitter is equipped with M_t transmit antennas and the receiver has a single antenna is considered. A unit norm beamforming vector (or beamformer) $\mathbf{f}_m \in \mathbb{C}^{M_t \times 1}$ at the mth channel instance is used to direct a symbol $s_m \in \mathbb{C}$ to the receiver. The symbol has $E[|s_m|^2] = 1$ for $m = 0, 1, \ldots$. The scalar received signal is represented by

$$y_m = \sqrt{\rho}\mathbf{h}_m^* \mathbf{f}_m s_m + w_m \tag{1}$$

where w_m denotes the additive noise distributed according to $\mathcal{CN}(0,1)$ and ρ represents the signal-to-noise ratio (SNR). Here, the channel $\mathbf{h}_m \in \mathbb{C}^{M_t \times 1}$ is a spatially uncorrelated flat fading channel and assumed invariant within the mth channel use (i.e., block fading channel). Each channel use could actually represent a block of channels. The time evolution is modeled by a first-order Gauss-Markov process [17]

$$\mathbf{h}_m = \epsilon \mathbf{h}_{m-1} + \sqrt{1-\epsilon^2}\mathbf{g}_m. \tag{2}$$

The $\mathbf{g}_m \in \mathbb{C}^{M_t \times 1}$ has i.i.d. entries distributed according to $\mathcal{CN}(0,1)$ and $E[\mathbf{h}_{m-1}\mathbf{g}_m^*] = \mathbf{0}_{M_t}$, where $\mathbf{0}_{M_t}$ denotes $M_t \times M_t$ zero matrix. The noise process w_m in (1) is assumed to be independent of $\mathbf{h}_0$ and $\mathbf{g}_m$, and $\mathbf{h}_0$ is independent of $\mathbf{g}_m$ for all $m \geq 1$. Here, the coefficient ϵ $(0 \leq \epsilon < 1)$ quantifies the amount of the correlation between elements $h_{m,i}$ and $h_{m+1,i}$, and we assume all the elements of $\mathbf{h}_m$ have the same time correlation coefficient ϵ. The condition $0 \leq \epsilon < 1$ is the basic assumption because the static case is unrealistic. The parameter ϵ can be selected to match the long term (e.g., second-order or beyond) statistics of physical channel propagation models. Using the popular Jakes' statistical model for fading channel [22] means that

$$\epsilon = J_0(2\pi f_D T) \tag{3}$$

where $J_0(\cdot)$ is the zeroth order Bessel function, T denotes the channel instantiation (or CSI feedback) interval, and $f_D = v f_c / c$ denotes the maximum Doppler frequency where v is the terminal velocity, f_c is the carrier frequency, and $c = 3 \times 10^8$ m/s. The long term statistic ϵ is perfectly known at the transmitter and receiver. Perfect CSI is available at the receiver side, while the transmitter has partial CSI attained from the reverse link (where the reverse link is error-free and zero-delay). Throughout the paper, the directions of $\mathbf{h}_m$ and $\mathbf{g}_m$ are denoted by $\tilde{\mathbf{h}}_m = \mathbf{h}_m/||\mathbf{h}_m||$ and $\tilde{\mathbf{g}}_m = \mathbf{g}_m/||\mathbf{g}_m||$, respectively.

In the channel model in (2), we focus on the scenario when the blocklength can span a large number of channel realizations. In this scenario, we can deal with ergodic capacity. This will mean that as ϵ gets closer to one the blocklength will have to increase. However, our interest is on the practical case when there is a

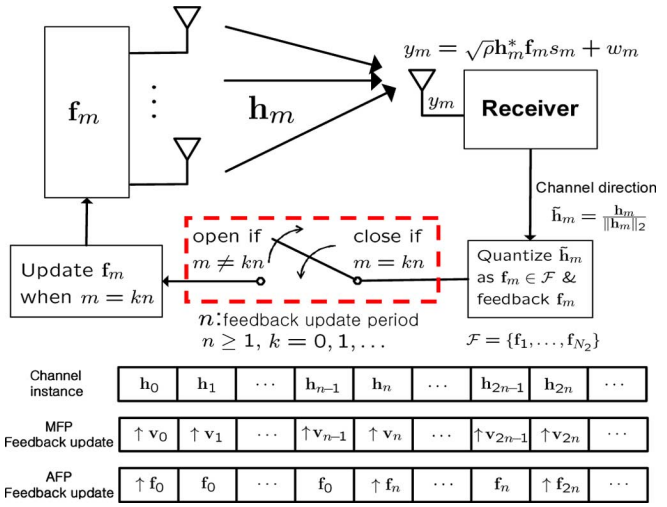

Fig. 1. Feedback frameworks for the MFP scheme and AFP scheme: *up arrow* ($\uparrow$) is used to indicate feedback update instance.

sufficient amount of mobility. This corresponds to the channel with ϵ substantially less than one.

Now, we present two feedback frameworks. The first one is a conventional limited feedback framework (e.g., [2]–[6]), and the second one is the feedback resource reusing scheme that can leverage the channel's temporal correlation. For future reference, we call the first feedback framework the minimum feedback period (MFP) scheme and the second feedback framework the adaptive feedback period (AFP) scheme.

1) MFP Scheme: At every channel instance m, the receiver uses a codebook $\mathcal{V} = \{\mathbf{v}_1, \mathbf{v}_2, \ldots, \mathbf{v}_{N_1}\}$ where $N_1 = 2^{B_1}$ and maximizes

$$\mathbf{v}_m = \arg\max_{\mathbf{v}\in\mathcal{V}} \left|\tilde{\mathbf{h}}_m^* \mathbf{v}\right|^2.$$

A random codebook is used to allow tractable analysis. At every m, the random codebook $\mathcal{V}$ is realized by choosing N_1 vectors independently from the uniform distribution on the M_t-dimensional unit sphere. At the receiver side, the normalized effective SNR is expressed by $\left|\mathbf{h}_m^* \mathbf{v}_m\right|^2$. Note that for the MFP scheme the feedback update period is 1 and the average feedback overhead is B_1 bits/channel use.

2) AFP Scheme: Similar to the MFP scheme, the AFP scheme employs a random beamforming codebook $\mathcal{F} = \{\mathbf{f}_1, \mathbf{f}_2, \ldots, \mathbf{f}_{N_2}\}$ with $N_2 = 2^{B_2}$. However, unlike the MFP scheme, the AFP scheme feeds back a beamformer index at every nth ($n \geq 1$) channel instance. Here, the positive integer n refers to feedback update period. Fig. 1 depicts the feedback frameworks for the MFP and AFP schemes. The *up arrow* ($\uparrow$) symbol is used to indicate an instance of feedback update. As can be seen from Fig. 1, at $m = 0$, the receiver of the AFP scheme feeds back the best beamformer index by finding

$$\mathbf{f}_0 = \arg\max_{\mathbf{f}\in\mathcal{F}} \left|\tilde{\mathbf{h}}_0^* \mathbf{f}\right|^2,$$

and $\mathbf{f}_0$ is used to transmit data at $m = 0$. The transmitter reuses $\mathbf{f}_0$ for channel instances $m = 1$ to $m = n - 1$, which is represented in Fig. 1 by $\mathbf{f}_0$ without $\uparrow$ from $m = 1$ to $m = n - 1$. From $m = 0$ to $m = n - 1$, the normalized effective SNR at the receiver side is $\left|\mathbf{h}_m^* \mathbf{f}_0\right|^2$. At $m = n$, the receiver sends back a new beamformer index by determining

$$\mathbf{f}_n = \arg\max_{\mathbf{f}\in\mathcal{F}} \left|\tilde{\mathbf{h}}_n^* \mathbf{f}\right|^2,$$

and $\mathbf{f}_n$ is reused during the next n times of transmissions.

In the AFP scheme, the feedback is only available at every nth channel instance. With this feedback setup, feeding back the best index with respect to the channel $\mathbf{h}_0$ and using $\mathbf{f}_0$ to transmit symbols for $m = 0$ to $m = n - 1$ can be justified by noting that the best linear predictor for the channel $\mathbf{h}_m$ (with $m \geq 1$) that the receiver can construct at $m = 0$ is $\hat{\mathbf{h}}_m = \epsilon^m \mathbf{h}_0$ in minimum mean square error (MMSE) sense. Using the model in (2), the receiver knows that at $m = 1$ the channel $\mathbf{h}_0$ will evolve to $\mathbf{h}_1$ by adding white excitation $\sqrt{1-\epsilon^2}\mathbf{g}_1$ to $\mathbf{h}_0$. The MMSE linear predictor is of the form $\hat{\mathbf{h}}_1 = \mathbf{A}\mathbf{h}_0$ where $\mathbf{A} \in \mathbb{C}^{M_t \times M_t}$. From the MMSE criterion, $\hat{\mathbf{h}}_1$ can be constructed by finding $\mathbf{A}$ such that

$$\mathbf{A} = \arg\min_{\tilde{\mathbf{A}}} E\left[\left\|\mathbf{h}_1 - \tilde{\mathbf{A}}\mathbf{h}_0\right\|_2^2\right].$$

It is well known that the optimal $\mathbf{A}$ in MMSE sense is given by $\mathbf{A} = E\left[\mathbf{h}_1 \mathbf{h}_0^*\right] \mathbf{R}_{\mathbf{h}_0}^{-1}$ where $\mathbf{R}_{\mathbf{h}_0} = E\left[\mathbf{h}_0 \mathbf{h}_0^*\right]$ in [23]. Since $\mathbf{R}_{\mathbf{h}_0} = \mathbf{I}_{M_t}$ and $E\left[\mathbf{h}_1 \mathbf{h}_0^*\right] = \epsilon \mathbf{I}_{M_t}$, the optimal MMSE linear predictor $\hat{\mathbf{h}}_1$ is given by $\epsilon \mathbf{h}_0$. At $m = 2$, given $\mathbf{h}_2 = \epsilon \mathbf{h}_1 + \sqrt{1-\epsilon^2}\mathbf{g}_2 = \epsilon^2 \mathbf{h}_0 + \sqrt{1-\epsilon^2}\left(\epsilon \mathbf{g}_1 + \mathbf{g}_2\right)$, the MMSE linear predictor is found as $\hat{\mathbf{h}}_2 = \epsilon^2 \mathbf{h}_0$. Repeated to $m = n - 1$, we readily obtain $\hat{\mathbf{h}}_m = \epsilon^m \mathbf{h}_0$. Then, the channel direction corresponding the MMSE predictors $\left\{\epsilon \mathbf{h}_0, \ldots, \epsilon^{n-1} \mathbf{h}_0\right\}$ is commonly given by $\tilde{\mathbf{h}}_0$ for time $m = 1$ to $m = n - 1$. The beamformer $\mathbf{f}_0$ results by quantizing $\tilde{\mathbf{h}}_0$ at $m = 0$.

The feedback update period n of the AFP scheme is fixed once online but can be adjusted offline to optimize some criterion that depends on the amount of channel correlation. If the channel fades slowly, the AFP scheme is amenable to control the feedback update period n to reduce the average feedback overhead while maintaining the performance greater than or equal to that of the MFP scheme. The benefits of the AFP scheme compared to the MFP scheme can be measured by the average feedback overhead and average performance. For this reason, we only are interested in comparing the MFP and AFP schemes when

$$\frac{B_2}{n} \leq B_1. \tag{4}$$

In addition, we also must require that $B_2 > B_1$ (or equivalently $N_2 > N_1$). Note that the scenario when $B_2 = B_1$ trivially leads to the AFP scheme and MFP scheme being equivalent.

The main findings of our work are as follows: 1) for fixed B_1, B_2 (with $B_2 > B_1$), and ϵ, we study what feedback update period guarantees that the AFP scheme outperforms the MFP scheme, 2) for fixed B_1 and B_2 (with $B_2 > B_1$), we determine the bound on ϵ guaranteeing that the AFP scheme dominates the MFP scheme, 3) for fixed N_1 and ϵ, we first determine $B_{2,\mathrm{opt}}$ and n_{opt} that maximize average effective SNR performance of the AFP scheme given fixed average feedback overhead $\gamma = B_2/n$ constraint and then, bound on $B_{2,\mathrm{opt}}$ is found such that the AFP scheme with $B_{2,\mathrm{opt}}$ and n_{opt} outperforms the MFP scheme with B_1, 4) for fixed N_1 and ϵ, we find the minimum required B_2 (i.e., $B_{2,\min}$) ensuring the update period n is greater

than or equal to a positive integer $\xi > 1$ while maintaining better performance than the MFP scheme. In general, we show that the average feedback overhead can be reduced by sending higher resolution feedback less frequently if the transmitter and receiver are not too mobile.

III. Bounds on Feedback Update Period and Feedback Rate

First, we derive bounds on the feedback update period n for the AFP scheme that ensure greater performance than the MFP scheme. Then, conditions on the correlation coefficient ϵ and the codebook size B_2 (feedback information rate of the AFP scheme) where the AFP scheme is beneficial over the MFP scheme in terms of the performance and average feedback overhead are characterized.

A. Bound on Feedback Update Period

At the mth channel instance, the normalized average effective SNR loss between the AFP scheme and the MFP scheme is defined by

$$\begin{aligned} D_m^{\text{snr}} &= E\left[|\mathbf{h}_m^*\mathbf{f}_0|^2 - |\mathbf{h}_m^*\mathbf{v}_m|^2\right] \\ &= E\left[\|\mathbf{h}_m\|^2\right] E\left[\left|\tilde{\mathbf{h}}_m^*\mathbf{f}_0\right|^2 - \left|\tilde{\mathbf{h}}_m^*\mathbf{v}_m\right|^2\right] \end{aligned} \tag{5}$$

where the equality in (5) is due to the independence between the channel amplitude $\|\mathbf{h}_m\|$ and the channel direction $\tilde{\mathbf{h}}_m$. Note that $E[\|\mathbf{h}_m\|^2] = M_t$.

Characterizing the feedback update period with D_m^{snr} in (5) requires closed-form expressions for $E[|\tilde{\mathbf{h}}_m^*\mathbf{f}_0|^2]$ and $E[|\tilde{\mathbf{h}}_m^*\mathbf{v}_m|^2]$. To evaluate the quantity $E[|\tilde{\mathbf{h}}_m^*\mathbf{v}_m|^2]$ of the MFP scheme, we use a random vector quantization result. It was shown in [18] that

$$E\left[\left|\tilde{\mathbf{h}}_m^*\mathbf{v}_m\right|^2\right] = 1 - N_1\beta\left(\frac{M_t}{M_t-1}, N_1\right) \tag{6}$$

where $\beta(a,b)$ is the beta function with parameter a and b. Interestingly, a related closed-form result for $E[|\tilde{\mathbf{h}}_m^*\mathbf{f}_0|^2]$ of the AFP scheme can be obtained.

Lemma 1: The quantity $E[|\tilde{\mathbf{h}}_m^*\mathbf{f}_0|^2]$ of the AFP scheme at the mth channel instance ($m \geq 0$) is given by

$$E\left[\left|\tilde{\mathbf{h}}_m^*\mathbf{f}_0\right|^2\right] = \epsilon^{2m}\left(1 - N_2\beta\left(\frac{M_t}{M_t-1}, N_2\right)\right) + \frac{1-\epsilon^{2m}}{M_t}. \tag{7}$$

Proof: See Appendix A. ∎

When $m = 0$, it is apparent that the right hand side (RHS) of (7) equals (6) with N_1 replaced by N_2. Note that as $m \longrightarrow \infty$, $E[|\tilde{\mathbf{h}}_m^*\mathbf{f}_0|^2] \longrightarrow 1/M_t$ implying (7) converges to a random beamforming gain $1/M_t$.

The quantity $N\beta(M_t/(M_t-1), N)$ stands for the average quantization error incurred by the random codebook with size N. This quantity has an equivalent product form

$$N\beta\left(\frac{M_t}{M_t-1}, N\right) = \prod_{i=1}^{N} \frac{i}{i + \frac{1}{M_t-1}}. \tag{8}$$

The details of (8) are provided in Appendix B. The equality (8) explicitly shows that $\lim_{M_t \longrightarrow \infty} N\beta(M_t/(M_t-1), N) = 1$ and $\lim_{N \longrightarrow \infty} N\beta(M_t/(M_t-1), N) = 0$ monotonically. This product formulation is important because it allows us to quantify the amount of gain obtained by adding one random codeword to a random codebook.

Now, let us define α_1 and α_2 as

$$\alpha_1 \triangleq N_1\beta\left(\frac{M_t}{M_t-1}, N_1\right) \quad \text{and} \quad \alpha_2 \triangleq N_2\beta\left(\frac{M_t}{M_t-1}, N_2\right)$$

respectively, where α_1 and α_2 denote the average quantization errors for the MFP and AFP schemes, respectively. Lemma 1 leads to a bound on the feedback update period n.

Theorem 1: Given $N_2 > N_1$, the feedback update period for the AFP scheme with random codebook $\mathcal{F}$ must satisfy

$$n \leq \left\lfloor \log_{\epsilon^2}\left(1 - \frac{\alpha_1 - \alpha_2}{\frac{M_t-1}{M_t} - \alpha_2}\right)\right\rfloor_+ + 1 \tag{9}$$

to provide an average effective SNR gain greater than or equal to the MFP scheme.

Proof: See Appendix C. ∎

The equality in (8) implies that for $N_2 > N_1 \geq 1$, we have a relation $M_t - 1/M_t \geq \alpha_1 > \alpha_2$ or equivalently $0 < (\alpha_1 - \alpha_2)/((M_t-1)/M_t - \alpha_2) \leq 1$. As α_2 decreases (i.e., as N_2 increases), the quantity $(\alpha_1 - \alpha_2)/((M_t-1)/M_t - \alpha_2)$ increases. Thus, with fixed N_1, it easily follows from Theorem 1 that in a highly correlated environment ($\epsilon \approx 1$), the AFP scheme can accommodate a large n with $N_2 > N_1$. For example, if $M_t = 4$, $B_2 = 6$, $B_1 = 4$, and $\epsilon = 0.99$, the upper bound in (9) returns $n \leq 14$.

A random codebook is employed because of its analytical amenability, and the MFP scheme is chosen to provide a reasonable comparison to the AFP scheme. In practice, the random codebook can be realized by sharing a common (and synchronized) source of randomness for generating codebooks between the transmitter and receiver. The value α_1 can be any value $\alpha_1' \geq 0$ that quantifies a threshold of the minimum performance gain that the AFP scheme with feedback update control can guarantee.

Consider a nonrandom and optimized (thereby fixed) codebook $\mathcal{G}$ obtained by minimizing the average quantization error, i.e.

$$\mathcal{G} = \underset{\tilde{\mathcal{G}}, |\tilde{\mathcal{G}}|=N}{\arg\min}\, E_{\mathbf{h}}\left[1 - \max_{\mathbf{g}\in\tilde{\mathcal{G}}} |\tilde{\mathbf{h}}^*\mathbf{g}|^2\right]. \tag{10}$$

When a fixed and optimized codebook (e.g., Lloyd codebook [2], [6], Grassmannian line packing [4], etc.) is used, the bound in (9) can still serve as a guide to control the feedback update period as shown in following Corollary.

Corollary 1: The bound on the feedback update period in (9) is a sufficient condition for the feedback update period of any optimized codebook $\mathcal{G}$ in (10).

Proof: Denote $\alpha_2' = E_{\mathbf{h}}\left[1 - \max_{\mathbf{g}\in\mathcal{G}} |\tilde{\mathbf{h}}^*\mathbf{g}|^2\right]$ as the quantization error incurred by the optimized codebook $\mathcal{G}$ with size N_2. Note that $\alpha_2 = E_{\mathcal{F}}\left[E_{\mathbf{h}|\mathcal{F}}\left[1 - \max_{\mathbf{f}\in\mathcal{F}} |\tilde{\mathbf{h}}^*\mathbf{f}|^2\right]\right]$. Since the average quantization error of an arbitrary codebook is lower bounded by that of an optimized codebook, i.e., $E_{\mathbf{h}|\mathcal{F}}\left[1 - \max_{\mathbf{f}\in\mathcal{F}} |\tilde{\mathbf{h}}^*\mathbf{f}|^2\right] \geq \alpha_2'$, taking expectation $E_{\mathcal{F}}[\cdot]$ to

both sides does not change the bound and results in $\alpha_2 \geq \alpha_2'$. This implies that with the threshold value $\alpha_1' \geq 0$ we have

$$\log_{\epsilon^2}\left(1-\frac{\alpha_1'-\alpha_2}{\frac{M_t-1}{M_t}-\alpha_2}\right) \leq \log_{\epsilon^2}\left(1-\frac{\alpha_1'-\alpha_2'}{\frac{M_t-1}{M_t}-\alpha_2'}\right). \tag{11}$$

Thus, from (11), it is apparent that (9) is the sufficient condition and can also be used to control the feedback update period for the optimized codebook. ■

Note that the bound in (11) is in fact tight because the random codebook performs measurably close to the optimized codebook [24].

B. Bound on Correlation Coefficient

For fixed N_1 and N_2 (with $N_2 > N_1$), in this subsection, Theorem 1 is reproduced to characterize the conditions on the time correlation coefficient ϵ that guarantee that the AFP scheme requires a smaller average feedback overhead than the MFP scheme while maintaining better performance than the MFP scheme. This characterization readily results in a switching criterion between the AFP and MFP schemes based on the time correlation coefficient ϵ.

Lemma 2: The AFP scheme achieves a larger average beamforming gain and uses a lower average feedback rate than the MFP scheme when the feedback update period n satisfies

$$\left\lceil \frac{B_2}{B_1} \right\rceil \leq n \leq \left\lfloor \log_{\epsilon^2}\left(1-\frac{\alpha_1-\alpha_2}{\frac{M_t-1}{M_t}-\alpha_2}\right)\right\rfloor_+ + 1. \tag{12}$$

Proof: The upper bound follows from Theorem 1, and the lower bound is due to the condition $B_2/n \leq B_1$, which is $\lceil B_2/B_1 \rceil \leq n$. Here, $\lceil \cdot \rceil$ denotes the ceiling function. ■

Also note that if the feedback update period is chosen such as $n \leq \lceil B_2/B_1 \rceil - 1$, there is no benefit of using the AFP scheme in terms of average feedback overhead, because n no longer satisfies (12). Thus, to investigate the operation of the AFP scheme, given $B_2 > B_1$, we find a condition for the correlation coefficient ϵ ensuring $n > \lceil B_2/B_1 \rceil - 1$. From Lemma 2, this condition is equivalent to

$$1-\frac{\alpha_1-\alpha_2}{\frac{M_t-1}{M_t}-\alpha_2} \leq \epsilon^{2(\lceil B_2/B_1\rceil-1)}$$

which is

$$\epsilon \geq \left(\frac{\frac{M_t-1}{M_t}-\alpha_1}{\frac{M_t-1}{M_t}-\alpha_2}\right)^{1/2(\lceil B_2/B_1\rceil-1)}. \tag{13}$$

Now, combining Lemma 2 and (13) gives a criterion for controlling the feedback update period.

Correlation Coefficient Criterion: *For fixed B_1 and B_2 with $B_2 > B_1$, the feedback update control for the AFP scheme outperforms the MFP scheme in terms of the average effective SNR performance and average feedback overhead when (12) and (13) are satisfied.*

This characterization specifies the minimum and maximum feedback update periods that the AFP scheme can achieve, if (13) satisfied. For instance, if $M_t = 4$, $B_1 = 4$ bits, and $B_2 = 6$ bits, the AFP scheme shows better performance with smaller average feedback overhead than the MFP scheme when $\epsilon \geq 0.872$. If $\epsilon = 0.982$, the AFP scheme has the feedback update period bound $2 \leq n \leq 8$. If we change $B_2 = 6$ bits to $B_2 = 8$ bits, the correlation coefficient criterion gives $\epsilon \geq 0.811$. When $\epsilon = 0.982$, the AFP scheme can utilize a feedback update period within $2 \leq n \leq 12$.

C. Bounds on Codebook Size

The codebook size of the AFP scheme has a significant impact on the average feedback overhead and performance. Choosing a large B_2 gives a significant performance gain but increases the average feedback overhead. A small B_2 decreases the average feedback overhead while degrades the performance. In this subsection, to find a tradeoff between the feedback rate B_2 and the feedback update period n, we first optimize B_2 and n so that the average effective SNR is maximized subject to $\gamma = B_2/n$. Our solution is based on a lower bound on the normalized average effective SNR gain where the bound allows us to compute the optimal B_2 and n in closed-form. Second, we find the minimum possible value of B_2 such that the AFP scheme with feedback update period $n = \xi$ outperforms the MFP scheme and gives smaller average feedback overhead than the MFP scheme.

1) Average Feedback Overhead Constraint: It is useful to review the bound [24]

$$\begin{aligned}\frac{M_t}{M_t-1}2^{-B/(M_t-1)} &\leq 2^B\beta\left(\frac{M_t}{M_t-1},2^B\right)\\ &\leq \Gamma\left(\frac{M_t}{M_t-1}\right)2^{-B/(M_t-1)}.\end{aligned} \tag{14}$$

From (14), the lower bound of (7) follows

$$\begin{aligned}&E\left[\left|\tilde{\mathbf{h}}_m^*\mathbf{f}_0\right|^2\right]\\ &\geq \epsilon^{2m}\left(\frac{M_t-1}{M_t}-\Gamma\left(\frac{M_t}{M_t-1}\right)2^{-B_2/(M_t-1)}\right)+\frac{1}{M_t}.\end{aligned} \tag{15}$$

However, the lower bound in (15) can be a negative value, implying it is not a properly defined quantity. Therefore, following condition must be assumed

$$\frac{M_t-1}{M_t}-\Gamma\left(\frac{M_t}{M_t-1}\right)2^{-B_2/(M_t-1)} \geq 0. \tag{16}$$

However, it can be readily shown that most of the feedback scenarios satisfy (16).

Lemma 3: If B_2 is chosen such that $B_2 \geq \log_2(e) \approx 1.443$, the bound in (16) always holds.

Proof: Using $\Gamma\left(M_t/(M_t-1)\right) \leq 1$, we further bound (16) as $(M_t-1)/M_t - 2^{-B_2/(M_t-1)} \geq 0$, which is equivalent to

$$B_2 \geq (M_t-1)\log_2\left(1+\frac{1}{M_t-1}\right). \tag{17}$$

Note that the RHS of (17) is an increasing function of M_t. Taking $M_t \rightarrow \infty$ to both sides of (17) and using the definition $\lim_{M_t\rightarrow\infty}\left(1+1/(M_t-1)\right)^{M_t-1} = e$ lead to the bound $B_2 \geq \log_2(e)$. ■

Remark 1: The bound in (15) is achieved as $B_2, M_t \rightarrow \infty$ and the ratio B_2/M_t converges to a bounded value. This is because the lower and upper bounds in (14) coincide as B_2, $M_t \rightarrow \infty$ while maintaining B_2/M_t to be bounded.

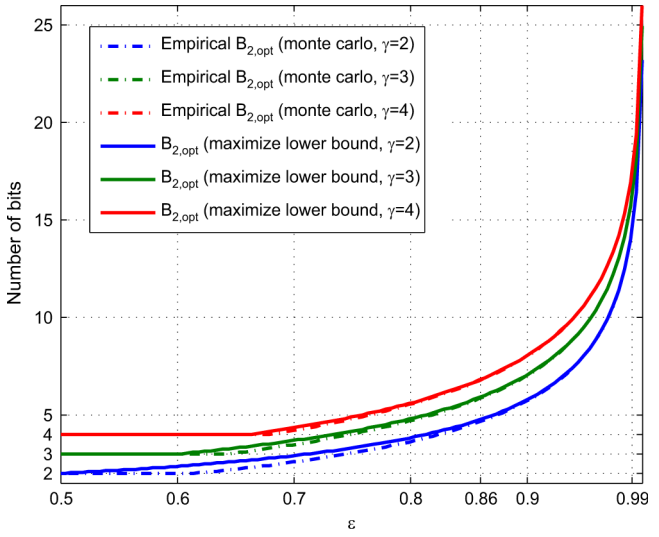

Fig. 2. $B_{2,\mathrm{opt}}$ obtained by maximizing the lower bound (19) versus Empirical $B_{2,\mathrm{opt}}$ obtained by monte carlo simulation so that (18) is maximized for $M_t = 4$ and $\gamma \in \{2,3,4\}$.

With $n = m+1$ and $\gamma = B_2/n$, the closed-form expression of $E[|\tilde{\mathbf{h}}_m^* \mathbf{f}_0|^2]$ in (7) and the lower bound in (15) are expressed in terms of B_2 and γ, and denoted by

$$F_{B_2,\gamma} = \epsilon^{2(B_2/\gamma-1)} \times \left(\frac{M_t-1}{M_t} - 2^{B_2}\beta\left(\frac{M_t}{M_t-1}, 2^{B_2}\right)\right) + \frac{1}{M_t} \quad (18)$$

and

$$G_{B_2,\gamma} = \epsilon^{2(B_2/\gamma-1)} \times \left(\frac{M_t-1}{M_t} - \Gamma\left(\frac{M_t}{M_t-1}\right)2^{-B_2/(M_t-1)}\right) + \frac{1}{M_t} \quad (19)$$

respectively. In addition, to satisfy the condition in Lemma 3 we assume that $\gamma \geq \log_2(e)$. The following lemma discusses finding the maximizer of $G_{B_2,\gamma}$ over B_2.

Lemma 4: Given an average feedback overhead constraint $\gamma = B_2/n \geq \log_2(e)$, the optimal B_2 that maximizes $G_{B_2,\gamma}$ is given by

$$B_{2,\mathrm{opt}} = (M_t-1) \times \log_2\left(\Gamma\left(1+\frac{M_t}{M_t-1}\right)\left(1+\gamma\frac{\ln 2^{-1/(M_t-1)}}{\ln \epsilon^2}\right)\right). \quad (20)$$

Proof: See Appendix D. ∎

With (20), the optimal feedback update period easily follows that $n_{\mathrm{opt}} = B_{2,\mathrm{opt}}/\gamma$. However, depending on ϵ, M_t, and γ values, it is possible that $B_{2,\mathrm{opt}}$ value in (20) returns $n_{\mathrm{opt}} < 1$. Note that $n_{\mathrm{opt}} < 1$ implies $m < 0$, which is impossible. In this trivial case, we choose $n = 1$ and $B_2 = \gamma$ (i.e., it becomes the MFP scheme). Fig. 2 displays $B_{2,\mathrm{opt}}$ and "Empirical $B_{2,\mathrm{opt}}$". The $B_{2,\mathrm{opt}}$ is obtained by (20) (with $B_{2,\mathrm{opt}} \geq \gamma$) and "Empirical $B_{2,\mathrm{opt}}$" is computed by monte carlo simulations so that (18) is maximized given $M_t = 4$ and $\gamma \in \{2,3,4\}$. Although (20) is based on the lower bound, it is suffice to claim the tightness of (19) from Fig. 2.

In Lemma 4, $B_{2,\mathrm{opt}}$ and n_{opt} are determined based on the performance of the AFP scheme. To characterize the benefits of the AFP scheme compared the MFP scheme, given the condition in (4) (i.e., $B_1 \geq \gamma$), we examine the condition for $B_{2,\mathrm{opt}}$ in (20) that ensures larger average effective SNR gain of the AFP scheme than that of the MFP scheme.

Theorem 2: The AFP scheme with $B_{2,\mathrm{opt}}$ in (20) and $n_{\mathrm{opt}} = B_{2,\mathrm{opt}}/\gamma$ provides a larger average effective SNR than the MFP scheme with $B_1 \geq \gamma$ and satisfies $n_{\mathrm{opt}} \geq 1$ if

$$\gamma \leq B_{2,\mathrm{opt}} \leq \frac{\ln \Phi}{\ln 2^{1/(M_t-1)} - \frac{1}{\gamma}\ln \epsilon^2} \quad (21)$$

where

$$\Phi = \left(\frac{\frac{\gamma}{M_t-1}\Gamma\left(\frac{M_t}{M_t-1}\right)}{\frac{M_t-1}{M_t} - \alpha_1}\right)\frac{\ln 2}{(-\epsilon^2 \ln \epsilon^2)}.$$

Proof: See Appendix E. ∎

The theorem establishes that if $B_{2,\mathrm{opt}}$ in (20) falls in the bound in (21), the average effective SNR performance of the proposed scheme always outperforms the MFP scheme with nontrivial feedback update period.

Remark 2: From (20), it is easy to check that the limit γ, $M_t \to \infty$ such that $\gamma/M_t = \kappa$ (with κ is bounded) implies that $B_{2,\mathrm{opt}}$, $M_t \to \infty$ such that $B_{2,\mathrm{opt}}/M_t$ is bounded. Therefore, from Remark 1, it is obvious that $B_{2,\mathrm{opt}}$ in (20) converges to the quantity B_2 that maximize $F_{B_2,\gamma}$ in (18) as $\gamma, M_t \to \infty$ such that $\gamma/M_t = \kappa$. This also implies that $G_{B_{2,\mathrm{opt}},\gamma}$ approaches the maximum of $F_{B,\gamma}$ and indeed $G_{B_{2,\mathrm{opt}},\gamma} \to F_{B_{2,\mathrm{opt}},\gamma}$.

The $B_{2,\mathrm{opt}}$ in (20) is the quantity that maximizes the average effective SNR gain. The $B_{2,\mathrm{opt}}$ in (20) grows large as $\epsilon \to 1$ so that it gives $E[|\tilde{\mathbf{h}}^* \mathbf{f}_0|^2] = 1$. Thus, when $\epsilon \approx 1$, $B_{2,\mathrm{opt}}$ in (20) gives an impractical large value. To put some number to (20), if $M_t = 4$, $\gamma = 4$, and $\epsilon = 0.99$, $B_{2,\mathrm{opt}}$ is given by 17.42 bits with $n_{\mathrm{opt}} = 4.36$.

2) Minimum Codebook Size: In the following, we find the minimum possible value of B_2 denoted by $B_{2,\min}$ such that given a positive integer $\xi > 1$ and B_1, the AFP scheme always shows better average effective SNR gain than the MFP scheme if $B_2 \geq B_{2,\min}$ and $n = \xi$.

Theorem 3: For a positive integer $\xi > 1$ and $B_1 \leq B_{1,\max}$ where

$$B_{1,\max} = \left\lfloor (M_t-1)\log_2\left(\frac{1}{1-\epsilon^{2(\xi-1)}}\right)\right\rfloor_+ \quad (22)$$

if B_2 is chosen such that $B_2 \geq B_{2,\min}$ where

$$B_{2,\min} = \left\lceil (M_t-1)\log_2\left(\frac{-\Gamma\left(1+\frac{M_t}{M_t-1}\right)\epsilon^{2(\xi-1)}}{\left(1-\epsilon^{2(\xi-1)}\right) - \frac{M_t}{M_t-1}\alpha_1}\right)\right\rceil_+ \quad (23)$$

the AFP scheme with feedback update period ξ yields a better average effective SNR gain than the MFP scheme.

Proof: See Appendix F. ∎

Theorem 3 shows how the minimum required feedback information rate of the AFP scheme should scale in terms of the required feedback update period and the amount of time correlation. When $\epsilon \approx 1$, the quantity inside of $\lceil\cdot\rceil_+$ in (23) is approximated as

$$\log_2\left(\frac{\Gamma\left(\frac{M_t}{M_t-1}\right)}{\alpha_1}\right)^{M_t-1}. \quad (24)$$

This indicates that in the slowly varying regime, the minimum required feedback rate $B_{2,\min}$ is not sensitive to the minimum

required feedback update period ξ. Thus, the AFP scheme should beneficially use a large feedback update period n when $\epsilon \approx 1$. However, as $\epsilon \longrightarrow 0$, the term $\epsilon^{2(\xi-1)}$ in (23) becomes dominant and the quantity inside of $\lceil\cdot\rceil_+$ in (23) is approximated as

$$(M_t-1)(\xi-1)\log_2\left(\frac{-\Gamma\left(1+\frac{M_t}{M_t-1}\right)\epsilon^2}{1-\frac{M_t}{M_t-1}\alpha_1}\right). \quad (25)$$

Note that (25) follows from the facts that the term $\epsilon^{2(\xi-1)}$ on the numerator inside of $\log_2(\cdot)$ scales linearly $B_{2,\min}$ in (23) with the $(\xi-1)$ term, but the term $\epsilon^{2(\xi-1)}$ on the denominator inside of $\log_2(\cdot)$ is negligible as $\epsilon \longrightarrow 0$.

When $\epsilon \approx 1$, $B_{1,\max}$ in (22) goes to infinity and B_1 becomes unconstrained. Thus, given a fixed B_1 and $\epsilon \approx 1$, from (24) and (14), it is not difficult to see that there exists $B_{2,\min}$ slightly greater than B_1 ensuring $n = \xi$. To put some numbers to (22) and (23), if $M_t = 4$, $\epsilon = 0.99$, and $\xi = 5$, $B_{1,\max}$ is given by 11 bits. If $B_1 = 5$ bits, then $B_2 \geq 6$ bits (i.e., $B_{2,\min} = 6$ bits). In this case, by designing the feedback with $B_2 = 6$ bits and $n = 5$ channel uses, the AFP scheme can operate with average feedback overhead 0.8 bits/channel use and outperform the MFP scheme which has an average feedback overhead of 4 bits/channel use. Compared to $B_{2,\text{opt}}$ and n_{opt} found by Theorem 2 where with $M_t = 4$, $\epsilon = 0.99$, $\gamma = 2$, and $B_1 = 5$ bits, it returns $B_{2,\text{opt}} = 14.51$ bits and $n_{\text{opt}} = 7.26$, finding the minimum required $B_{2,\min}$ and ξ gives practical insight for controlling feedback.

D. Capacity

As well as effective SNR, capacity is also an important quantity to measure the performance and is closely related to the effective SNR performance. The average capacity difference between the MFP and AFP schemes is given by

$$D_m^{\text{cap}} = E\left[\log_2\left(1+\rho\left|\mathbf{h}_m^*\mathbf{f}_0\right|^2\right)-\log_2\left(1+\rho\left|\mathbf{h}_m^*\mathbf{v}_m\right|^2\right)\right]. \quad (26)$$

For the quantized beamforming system, a closed-form expression for the average capacity is challenging if not impossible to determine. In this subsection, we deal with the nonasymptotic behavior as a function of the feedback update period. To provide a rule of thumb for controlling the feedback update period, note that a lower bound on D_m^{cap} is

$$\begin{aligned} D_m^{\text{cap}} &= E\left[\log_2\left(1+\frac{\rho\left\|\mathbf{h}_m\right\|^2\left(\left|\tilde{\mathbf{h}}_m^*\mathbf{f}_0\right|^2-\left|\tilde{\mathbf{h}}_m^*\mathbf{v}_m\right|^2\right)}{1+\rho\left\|\mathbf{h}_m\right\|^2\left|\tilde{\mathbf{h}}_m^*\mathbf{v}_m\right|^2}\right)\right] \\ &\geq \log_2(e)E\left[\frac{\rho\left\|\mathbf{h}_m\right\|^2\left(\left|\tilde{\mathbf{h}}_m^*\mathbf{f}_0\right|^2-(1-\alpha_1)\right)}{1+\rho\left\|\mathbf{h}_m\right\|^2\left|\tilde{\mathbf{h}}_m^*\mathbf{f}_0\right|^2}\right] \end{aligned} \quad (27)$$

where (27) follows from the bound $\ln(1+x) \geq x/(1+x)$ for $x > -1$ and $E[|\tilde{\mathbf{h}}_m^*\mathbf{v}_m|^2] = 1-\alpha_1$. Note that the bound in (27) gives a sufficient condition on the feedback update period. The distortion in (27) can then be further analyzed at both low and high SNR.

At low SNR, (27) becomes

$$D_m^{\text{cap}} \overset{\rho\longrightarrow 0}{\gtrsim} \log_2(e)\left(\rho M_t\right)E\left[\left|\tilde{\mathbf{h}}_m^*\mathbf{f}_0\right|^2-(1-\alpha_1)\right] \triangleq D_{m,\text{low}}^{\text{cap}}. \quad (28)$$

The expression in (28) implies $D_{m,\text{low}}^{\text{cap}} = \log_2(e)\rho D_m^{\text{snr}}$. Therefore, Theorem 1 characterizes a sufficient condition for the feedback update period necessary for capacity performance of the AFP scheme to meet or exceed capacity performance of the MFP scheme at low SNR.

Using (27) and high SNR analysis, we further get

$$\begin{aligned} D_m^{\text{cap}} &\overset{\rho\longrightarrow\infty}{\gtrsim} \log_2(e)E\left[1-\frac{1-\alpha_1}{\left|\tilde{\mathbf{h}}_m^*\mathbf{f}_0\right|^2}\right] \\ &\gtrsim \log_2(e)E\left[1-(1-\alpha_1)\left(1+2\left(1-\left|\tilde{\mathbf{h}}_m^*\mathbf{f}_0\right|^2\right)\right)\right] \\ &\triangleq D_{m,\text{high}}^{\text{cap}} \end{aligned} \quad (29)$$

where in (29) we use the expansion $1/a = 1+(1-a)+(1-a)^2+\cdots$ for $a \in [0,1]$ and take the first three terms $1/a \approx 1+(1-a)+(1-a)^2 \leq 1+2(1-a)$, which is accurate when a is close to 1. Thus, the optimization problem is formulated as

$$m = \underset{\tilde{m}\ \text{s.t.}\ D_{\tilde{m},\text{high}}^{\text{cap}}\geq 0}{\arg\min} D_{\tilde{m},\text{high}}^{\text{cap}}. \quad (30)$$

After manipulating (29) with the constraint $D_{\tilde{m},\text{high}}^{\text{cap}} \geq 0$ and $n = m+1$, a bound on the feedback update period at high SNR is

$$n \overset{\text{high}}{\lesssim} \left\lfloor \log_{\epsilon^2}\left(1-\frac{\frac{\alpha_1}{2(1-\alpha_1)}-\alpha_2}{\frac{M_t-1}{M_t}-\alpha_2}\right)\right\rfloor_+ + 1. \quad (31)$$

Comparing the bounds in (9) and (31), if $\alpha_1/2(1-\alpha_1) \leq \alpha_1$ (i.e., $\alpha_1 \leq 1/2$), the bound in (31) yields a smaller maximum update period than the bound in (9). This implies that if $\alpha_1 \leq 1/2$, the AFP scheme operating in the high SNR regime yields a smaller maximum update period than the AFP scheme operating at low SNR. The condition $\alpha_1 \leq 1/2$ is always satisfied if $B_1 \geq M_t - 1$. To see this, consider the upper bounds $\alpha_1 \leq \Gamma(M_t/(M_t-1))2^{-B_1/(M_t-1)} \leq 2^{-B_1/(M_t-1)}$. The bound $\alpha_1 \leq 2^{-B_1/M_t-1}$ indicates that for any $B_1 \in [M_t-1,\infty)$, α_1 is always upper bounded by $1/2$ (i.e., $\alpha_1 \leq 1/2$). Thus, given $B_1 \geq (M_t-1)$, a sufficient condition on the feedback update period to guarantee that the AFP scheme provides a larger ergodic capacity than the MFP scheme is given by (31).

IV. Asymptotic Analysis

For the case of effective SNR, it was possible to derive closed-form expressions and characterize the behavior of the AFP scheme with different feedback design parameters (e.g., feedback update period, time correlation coefficient, and required feedback rate). However, for the capacity criterion, only approximated bounds have been considered. In this section, bounds on the feedback update periods for the two performance (capacity and effective SNR) criteria are evaluated in the large system limit as the number of antennas M_t and feedback bits

B tend to infinity while maintaining fixed ratio $a = M_t/B$. For notational simplicity, we drop the subscript on B_2 of the AFP scheme. The dropped subscript will reappear at the end of the section. The purpose of asymptotic analysis is to provide practical insight rather than an implementation framework. The presented analysis provides the convergence trends of the feedback update period associated with the two different metrics. Simulation results provided in Section V demonstrate that these asymptotic trends are actually quite relevant even for reasonable numbers of antennas and feedback bits. It is shown that the update period bounds for the two criteria indeed converge to the same bound in the large system limit. To verify this, we first characterize the convergence rule of the instantaneous beamforming gain of the AFP scheme in the large system limit. Then, this result leads to the convergence of the two performance criteria.

For a size $N = 2^B$ random vector codebook $\mathcal{V} = \{\mathbf{v}_1, \ldots, \mathbf{v}_N\}$ with isotropically distributed $\mathbf{v}_i \in \mathbb{C}^{M_t \times 1}$ and $\|\mathbf{v}_i\| = 1$, the distribution function of $|\tilde{\mathbf{h}}_m^* \mathbf{v}_i|^2$ is given by [4]

$$\Pr\left(\left|\tilde{\mathbf{h}}_m^* \mathbf{v}_i\right|^2 \le x\right) = 1 - (1-x)^{M_t - 1}.$$

Letting $M_t = aB$, the distribution function of the max order statistic $X_B = \max_{\mathbf{v}\in\mathcal{V}} |\tilde{\mathbf{h}}_m^* \mathbf{v}|^2$ is

$$F_{X_B}(x) = \left(1 - (1-x)^{aB-1}\right)^{2^B}. \tag{32}$$

Now, the limiting behavior of $F_{X_B}(x)$ as $(M_t, B) \longrightarrow \infty$ is of interest.

Lemma 5: As B, $M_t \longrightarrow \infty$ while maintaining $a = M_t/B$, the distribution function $F_{X_B}(x)$ in (32), converges pointwise to

$$F_{X_\infty}(x) = \begin{cases} 0 & \text{if } 0 \le x < 1 - 2^{-1/a} \\ e^{-2^{1/a}} & \text{if } x = 1 - 2^{-1/a} \\ 1 & \text{if } 1 - 2^{-1/a} < x \le 1. \end{cases} \tag{33}$$

Proof: See Appendix G. ∎

Note that the convergence $F_{X_B}(x) \longrightarrow F_{X_\infty}(x)$ in (33) is pointwise because of the single discontinuity at $x = 1 - 2^{-1/a}$. Obviously, on the open intervals $\left[0, 1 - 2^{-1/a}\right)$ and $\left(1 - 2^{-1/a}, 1\right]$, the convergence is uniform. In Fig. 3, the distribution function (32) is displayed for $B \in \{2, 8, 32, 128\}$ with ratio $1 = a = M_t/B$. As can be seen from Fig. 3, the probability of X_B tends to concentrate around $x = 1 - 2^{-1/a} = 1/2$ as $(B, M_t) \longrightarrow \infty$.

The bound in (14) reveals that as B, $M_t \longrightarrow \infty$ with $a = M_t/B$, $E[X_B]$ converges to $1 - 2^{-1/a}$. The fact $E[X_B] \longrightarrow 1 - 2^{-1/a}$ and the limiting distribution in Lemma 5 together claim the convergence of the random variable $X_B \longrightarrow 1 - 2^{-1/a}$ as B, $M_t \longrightarrow \infty$.

Lemma 6: If B, $M_t \longrightarrow \infty$ with $a = M_t/B$, then X_B converges as [25]

$$X_B \xrightarrow{\text{m.s.}} 1 - 2^{-1/a} \tag{34}$$

in mean-square sense.

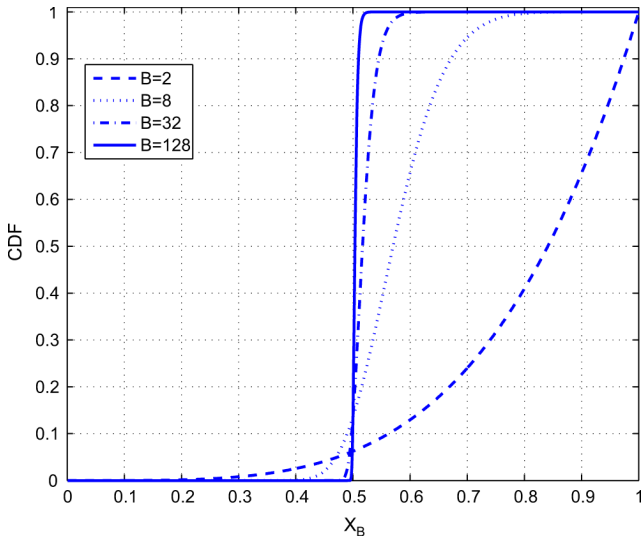

Fig. 3. Cumulative distribution function (CDF) of $F_{X_B}(x)$ in (32) for $B = 2, 8, 32, 128$ such that $1 = M_t/B$.

While the derivation for (34) in [25] relies on extreme order statistics, this result can be tractably verified using Lemma 5, as provided in Appendix H.

Characterizing the feedback update period for the AFP scheme in the large system limit requires analysis of the behavior of $\left|\tilde{\mathbf{h}}_m^* \mathbf{f}_0\right|^2$ as B, $M_t \longrightarrow \infty$.

Lemma 7: If B, $M_t \longrightarrow \infty$ in such a way that $a = M_t/B$, then the quantity $\left|\tilde{\mathbf{h}}_m^* \mathbf{f}_0\right|^2$ of the AFP scheme converges as

$$\left|\tilde{\mathbf{h}}_m^* \mathbf{f}_0\right|^2 \xrightarrow{\text{m.s.}} \epsilon^{2m}\left(1 - 2^{-1/a}\right) \tag{35}$$

in mean-squared sense.

Proof: See Appendix I. ∎

In the large system limits, $|\tilde{\mathbf{h}}_m^* \mathbf{f}_0|^2$ of the AFP scheme scales linearly with ϵ^2 and exponentially with the channel use index m. Denote the feedback update periods of the AFP scheme for the effective SNR and capacity difference functions in the large system limit as $n_{\infty,\text{snr}}$ and $n_{\infty,\text{cap}}$, respectively. Then, Lemma 7 enables us to characterize feedback update period bounds for the effective SNR and capacity in closed form and show that two performance criteria are closely related each other.

Theorem 4: As B_1, B_2, $M_t \longrightarrow \infty$ in such a way that $a_1 = M_t/B_1$ and $a_2 = M_t/B_2$, the feedback update periods $n_{\infty,\text{snr}}$ and $n_{\infty,\text{cap}}$ for the AFP scheme ensuring greater average effective SNR and capacity performance than the MFP scheme converge to a bound

$$n_{\infty,\text{snr}} = n_{\infty,\text{cap}} \overset{\text{m.s.}}{\le} \left\lfloor \log_{\epsilon^2}\left(\frac{1 - 2^{-1/a_1}}{1 - 2^{-1/a_2}}\right)\right\rfloor_+ + 1 \tag{36}$$

in mean-square sense.

Proof: See Appendix J. ∎

The inherent ρ dependency on the feedback update period with the capacity loss (which is studied in Section III-D) vanishes as $B_1, B_2, M_t \longrightarrow \infty$, and the bound converges to the same

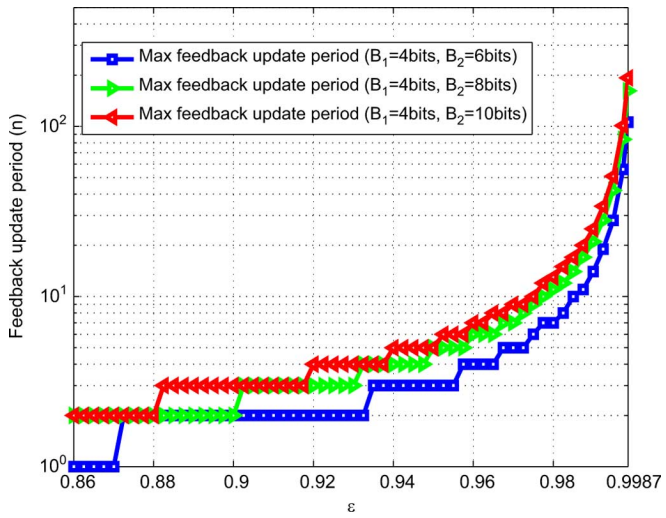

Fig. 4. Maximum achievable feedback update period of the AFP scheme for $B_1 = 4$ and $B_2 = 6, 8, 10$.

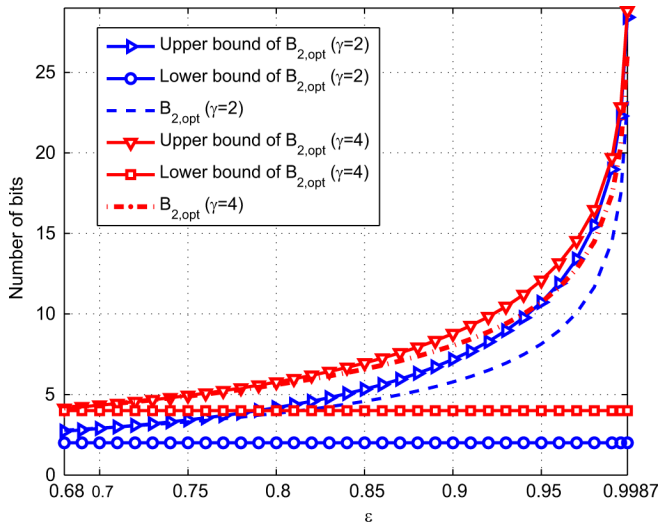

Fig. 5. Upper bound and lower bound in (21) with $B_{2,\mathrm{opt}}$ in (20) for different average feedback overhead using $\gamma = 2, 4$, $M_t = 4$, and $B_1 = \gamma$.

bound as the effective SNR criterion. This verifies that the intuition that the two performance metrics are asymptotically equivalent.

V. Numerical Simulations

In this section, we provide numerical results to corroborate the theorems in the previous sections. These results are from Monte Carlo simulations designed to evaluate the performance of the AFP and MFP schemes. As we have specified in (3), the correlation coefficient ϵ was generated using Jakes' model, i.e., $\epsilon = J_0(2\pi f_D T)$. To provide a meaningful comparison, we used practical parameters from IEEE Standard 802.16m [26]. In [26], the closed-loop operation assumes a terminal speed of 3 km/h with a CSI feedback interval of $T = 5$ ms and carrier frequency of $f_c = 2.5$ GHz. We use the above system parameters to simulate. Then, the temporal correlation variable ϵ varies from 0.9987 to 0.8721 as the terminal speed varies from 1 km/h to 10 km/h.

Fig. 4 displays the maximum feedback update period using (9) with $M_t = 4$, $B_1 = 4$ bits, and $B_2 \in \{6, 8, 10\}$ bits. The temporal correlation variable ϵ varies from 0.86 (11 km/h) to 0.9987 (1 km/h). As can be seen from Fig. 4, as ϵ approaches 1, the growth rate of the maximum feedback update period using the effective SNR criterion increases exponentially. When $B_2 = 6$ bits and $\epsilon = 0.9881$ (3 km/h) in Fig. 4, the AFP scheme can reuse the initial 6 bits of feedback up to 13 channel uses (i.e., the average feedback overhead is 0.46 bits/channel use), while assuring that the average effective SNR for the AFP scheme is larger than that of the MFP scheme. When $\epsilon = 0.9987$ (1 km/h), the AFP scheme can send back 6 bits of CSI every 106 channel uses (i.e., the average feedback overhead is 0.06 bits/channel use). Note that in any case, the average feedback overhead of the MFP scheme is 4 bits/channel use. The *Correlation Coefficient Criterion* in Section III-B reveals that the AFP scheme is initiated and ensures a lower average feedback overhead and greater effective SNR gain than the MFP scheme, if $\epsilon \geq 0.872$, when $B_2 = 6$ bits. In the same manner, when $B_2 = 10$ bits, the feedback update control is initiated when $\epsilon \geq 0.882$.

Fig. 5 displays the upper bound and lower bound in (21) and the feedback rate $B_{2,\mathrm{opt}}$ in (20) with different values of $(\gamma = 2, B_1 = 2$ bits) and $(\gamma = 4, B_1 = 4$ bits) for $M_t = 4$. The γ values are chosen to satisfy $\gamma \geq \log_2(e)$ due to lemma 3. As can be seen from the figure, for $\gamma = 2$ and $B_1 = 2$ bits, if $\epsilon \geq 0.72$ (15 km/h) the AFP scheme with $B_{2,\mathrm{opt}}$ in (20) shows improved performance than the MFP scheme with $B_1 = 2$ bits. Similarly, for $\gamma = 4$ and $B_1 = 4$ bits, when $\epsilon \geq 0.68$ (18 km/h) the proposed scheme shows benefits in terms of the average feedback overhead and performance compared to the MFP scheme with $B_1 = 4$ bits. As shown in Fig. 2, when $\epsilon \approx 1$, $B_{2,\mathrm{opt}}$ gives unintended large value of $B_{2,\mathrm{opt}}$. As can be seen from the next simulation study, finding the minimum codebook size $B_{2,\min}$ in (23) gives more practical insights than $B_{2,\mathrm{opt}}$.

Fig. 6 displays $B_{1,\max}$ (22) and $B_{2,\min}$ in (23) for $M_t = 4$ and $\xi \in \{2, 3\}$. Note that $B_{2,\min}$ for $\xi \in \{2, 3\}$ have been plotted by setting $B_1 = 4$ bits. For the $\xi = 2$ case, Fig. 6 shows $B_1 = 4$ bits satisfies $B_1 \leq B_{1,\max}$ for $0.86 \leq \epsilon \leq 0.9987$. For the $\xi = 3$ case, $B_1 = 4$ bits satisfies $B_1 \leq B_{1,\max}$ for $0.882 \leq \epsilon \leq 0.9987$. As ϵ tends to one, Fig. 6 demonstrates that B_1 is roughly unconstrained. The feedback bound $B_{2,\min}$, which guarantees the feedback update period ξ, is inversely proportional to ϵ. As investigated in Section III-C, $B_{2,\min}$ is not affected by the change of ξ at $\epsilon \approx 1$. However, $B_{2,\min}$ almost linearly scales with ξ when $\epsilon < 0.92$. If $\xi = 2$ and $\epsilon = 0.872$, $B_{1,\max}$ in (22) and $B_{2,\min}$ in (23) return $B_{2,\min} = 6$ bits and $B_{1,\max} = 6$ bits. Then, Theorem 3 indicates that with these parameters, the AFP scheme using $B_2 = 6$ bits and $n = 2$ is beneficial over the MFP scheme with $B_1 = 5$ bits when $\epsilon = 0.872$. In addition, from the *Correlation Coefficient Criterion*, when $\epsilon \geq 0.872$, we can choose $n \geq 2$ satisfying (12) so that the average feedback overhead of the AFP scheme is less than or equal to $B_2/\xi = 3$ bits/channel use. For the $\xi = 3$ case, the AFP scheme with $B_2 = 10$ bits outperforms the MFP scheme with $B_1 = 4$ bits when $\epsilon = 0.882$. In addition, the *Correlation Coefficient Criterion* indicates that the AFP scheme can always

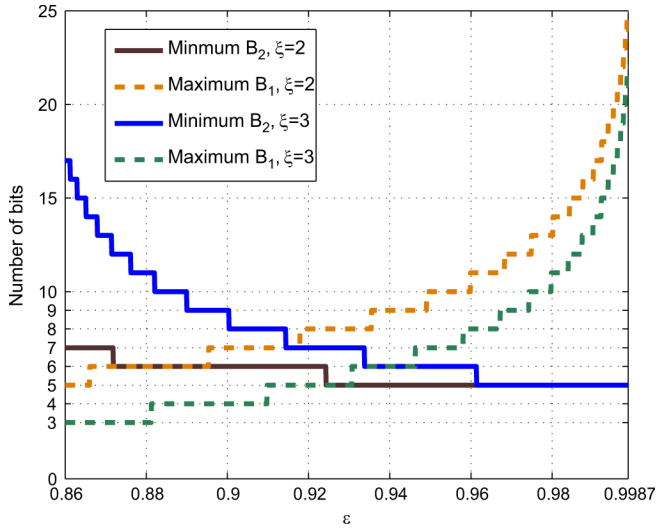

Fig. 6. Codebook sizes $B_{2,\min}$ in (23) and $B_{1,\max}$ in (22) ensuring $n = \xi$ for $M_t = 4$.

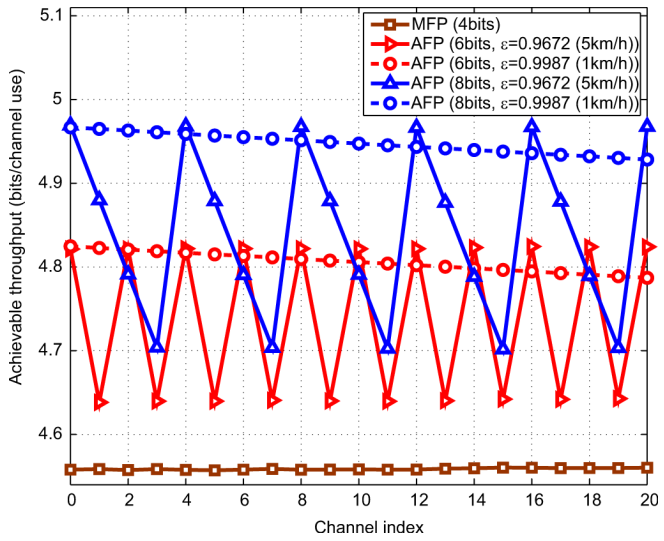

Fig. 8. Achievable throughput performance for the MFP and AFP schemes where the feedback update period is determined by the upper bound in (31).

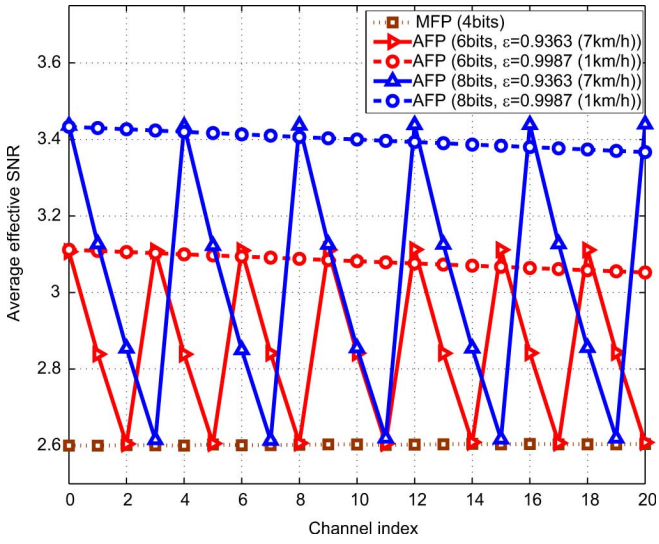

Fig. 7. Effective SNR performances for the MFP and AFP schemes where the feedback update period is determined by the upper bound in (9).

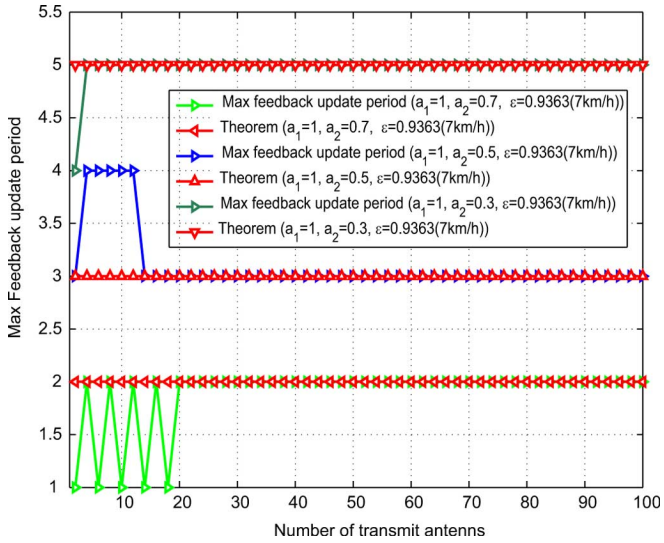

Fig. 9. Convergence of feedback update period as M_t, B_1, $B_2 \to \infty$ maintaining $a_1 = M_t/B_1$ and $a_2 = M_t/B_2$ ($\epsilon = 0.9363$ (7 km/h)).

be operated so that the average feedback overhead is less than or equal to $B_2/\xi = 3.33$ bits/channel use when $\epsilon \geq 0.882$.

Fig. 7 displays the average effective SNR across channel use index. $B_1 = 4$ bits and $B_2 \in \{6, 8\}$ bits are chosen to meet the conditions in (22) and (23), respectively (with $\xi = 2$). The feedback update periods of the AFP scheme are set by the maximum available update period in (9). As is shown in Fig. 7, a feedback update control criterion characterizes the feedback update period required to guarantee a larger effective SNR gain and lower feedback overhead rate than the MFP scheme. Fig. 8 displays the achievable throughput evaluated at each channel use index where the feedback update period is determined by (31). The bound in (31) is an approximation, but it gives insight into the feedback update period allowed. Figs. 7 and 8 reveal that as ϵ increases, the AFP scheme achieves a greater performance gain with significantly reduced average feedback overhead.

In this simulation study, we investigated the convergence result in Theorem 4. For this purpose, Fig. 9 demonstrates the maximum allowed feedback update period in Theorem 1 across different numbers of transmit antennas for $a_1 = 1$ and $a_2 \in \{0.7, 0.5, 0.3\}$ maintaining $a_1 = M_t/B_1$ and $a_2 = M_t/B_2$ and check that the bound in (9) converges to (36). In Fig. 9, the label "Theorem" denotes the maximum feedback update period in (36). Fig. 9 displays the mean-square convergence of (9) to the limiting bound in (36) for $\epsilon = 0.9363$ (or 7 km/h) and indicates that the convergence is indeed fast.

In this simulation study, the normalized effective SNR performance of the AFP scheme is compared to differential feedback schemes in [8] and [14] for $M_t = 4$ beamforming system. To quantize the initial state $\mathbf{f}_0$ we use a 4 bits of Grassmannian line packing codebook [4] for [8], [14] and after the first feedback, a 4 bits Gaussian vector quantization (VQ) codebook [8] and 4 bits rotation codebook [14] are used to feed back the channel variation. Gaussian VQ is used to quantize the angular velocity matrix to construct points on the geodesic lines defined on Grassmannian manifold in [8]. The length of the arc

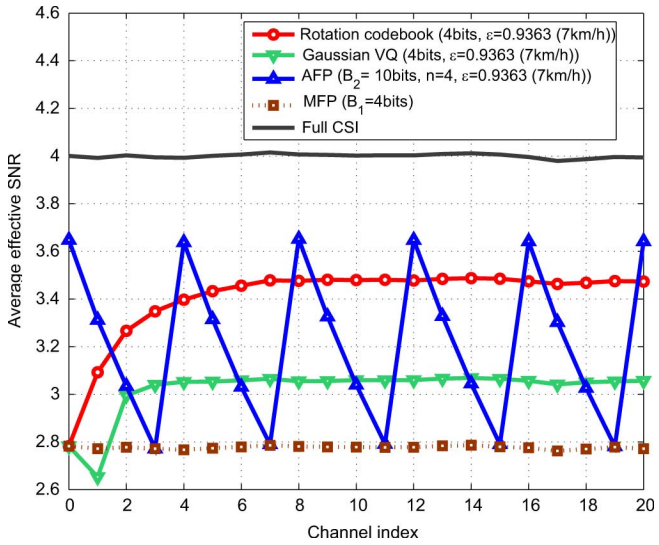

Fig. 10. Effective SNR performances for the AFP scheme, the MFP scheme, and differential feedback approaches in [8] and [14].

of geodesic is specified by a parameter $a \geq 0$ which impact the performance of the algorithm. Eight order polynomial in [8] is employed to provide appropriate a value with respect to the terminal speed. Fig. 10 shows the normalized effective SNR performance of the AFP scheme, the MFP scheme, and differential feedback schemes in [8], [14] with $\epsilon = 0.9363$ (or 7 km/h). For the AFP scheme, $B_2 = 10$ and $n = 4$ are used to give compatible performance to [8], [14]. The values $B_2 = 10$ and $n = 4$ are chosen based on Theorem 3. The average feedback overhead of the AFP scheme is 2.5 bits/channel use whereas the MFP scheme and differential strategies correspond to 4 bits/channeluse. The AFP scheme outperforms Gaussian VQ for the first two channel instances and shows better performance than rotation codebook only for the first channel instances. The gain of the differential feedback comes from the refinement algorithm operating in every channel instances and consecutive feedback to refine quantizer for every channel uses. The merits of the AFP scheme are its simplicity which does not require prediction and consecutive feedback for every channel uses.

VI. Conclusions and Discussions

In this paper, we derived a feedback reuse criterion for a limited feedback beamforming system. By computing the closed form expression of the average effective SNR, the feedback update period of the AFP scheme was identified. Based on this statistic, we determined how the feedback update period and the required codebook size should scale with the amount of temporal correlation. Through an asymptotic study, it was shown that the bounds on the feedback update period for the effective SNR and capacity performance converge to the same bound. From the simulation study, the proposed feedback update control framework showed improved performance with reduced average feedback overhead. These results reveal the necessity of taking temporal correlation into account during feedback design and demonstrates that infrequent high resolution feedback is preferable to frequent low resolution feedback if the terminals are not too mobile

The channel was assumed to follow a block fading model with temporally correlated blocks. Using an error-free and zero-delay feedback channel, we compared the MFP and AFP schemes. Even if we change the block fading assumption so that channel remains the same for a few symbols (say L symbols), the results in this paper do not change as long as our interest is in comparing the MFP and AFP schemes at the last channel use (in order to guarantee that AFP gives average effective SNR enhancement at every channel use). The only difference comes from the scaling factor L where the average feedback overheads of the MFP scheme and AFP scheme become B_1/L and $B_2/(nL)$, respectively, whose relative relation for comparing the performance does not change.

We assumed the feedback is only available at every nth channel instances for the AFP scheme. We did not assume any additional feedback to the transmitter between $m = 1$ and $m = n - 1$. If a prediction scheme operating at the transmitter is employed so that after the first transmission, the transmitter can predict a good beamformer using additional feedback side information at $m = 1$, then using a refined beamformer from time $m = 1$ to $m = n - 1$ may give better performance than simply using $\mathbf{f}_0$ from $m = 0$ to $m = n - 1$. There are many prediction approaches such as [7]–[9] to refine the initial quantizer $\mathbf{f}_0$ using a small amount of feedback. Incorporating a decent prediction algorithm is an interesting topic for future research on feedback update control.

Finally, one limitation of the work is that we considered only the feedback update control problem for single user beamforming. It is well known that MIMO channel can increase sum capacity by supporting multiple-users for downlink. Similar analysis may be directly applicable to multi-user beamforming because in that case the interest also is in maximizing the inner product between the channel vector and the quantized channel. In the general multiuser case, the feedback update period and necessary feedback rate will be determined by the most mobile user. Developing a user scheduling framework that uses feedback and takes into account the temporal correlation of the channel is an interesting topic for future work.

Appendix A
Proof of Lemma 1

Trivially, at $m = 0$, the average effective SNR of the AFP scheme is given by $E[|\mathbf{h}_0^* \mathbf{f}_0|^2]$. At $m = 1$, we have

$$E\left[|\mathbf{h}_1^* \mathbf{f}_0|^2\right] = E\left[\left|\left(\epsilon \mathbf{h}_0 + \sqrt{1-\epsilon^2}\mathbf{g}_1\right)^* \mathbf{f}_0\right|^2\right] = \epsilon^2 E\left[|\mathbf{h}_0^* \mathbf{f}_0|^2\right] + \left(1-\epsilon^2\right) E\left[|\mathbf{g}_1^* \mathbf{f}_0|^2\right] \quad (37)$$

where (37) follows from the facts that $\mathbf{h}_0$ and $\mathbf{g}_1$ are independent and have zero mean, and thereby the expectations of all cross-terms become $E[\mathbf{f}_0^* \mathbf{h}_0 \mathbf{g}_1^* \mathbf{f}_0] = E[\mathbf{f}_0^* \mathbf{g}_1 \mathbf{h}_0^* \mathbf{f}_0] = 0$. Similarly, when $m = 2$

$$E\left[|\mathbf{h}_2^* \mathbf{f}_0|^2\right] = \epsilon^2 E\left[|\mathbf{h}_1^* \mathbf{f}_0|^2\right] + \left(1-\epsilon^2\right) E\left[|\mathbf{g}_2^* \mathbf{f}_0|^2\right] \quad (38)$$

$$= \epsilon^4 E\left[|\mathbf{h}_0^* \mathbf{f}_0|^2\right] + \left(1-\epsilon^2\right) \sum_{i=0}^{1} \epsilon^{2i} E\left[|\mathbf{g}_{2-i}^* \mathbf{f}_0|^2\right] \quad (39)$$

where (39) is obtained by plugging (37) in (38). Then, it is straightforward, for a general m

$$E\left[\left|\mathbf{h}_m^*\mathbf{f}_0\right|^2\right] = \epsilon^{2m}E\left[\left|\mathbf{h}_0^*\mathbf{f}_0\right|^2\right] + \left(1-\epsilon^2\right)\sum_{i=0}^{m-1}\epsilon^{2i}E\left[\left|\mathbf{g}_{m-i}^*\mathbf{f}_0\right|^2\right].$$

Noting the independence between the directions and the amplitudes of $\mathbf{h}_m$ and $\mathbf{g}_{m-i}$ and using the fact that the amplitudes satisfy $E\left[\|\mathbf{h}_m\|^2\right] = E\left[\|\mathbf{g}_{m-i}\|^2\right] = M_t$ yield

$$E\left[\left|\tilde{\mathbf{h}}_m^*\mathbf{f}_0\right|^2\right] = \epsilon^{2m}E\left[\left|\tilde{\mathbf{h}}_0^*\mathbf{f}_0\right|^2\right] + \left(1-\epsilon^2\right)\sum_{i=0}^{m-1}\epsilon^{2i}E\left[\left|\tilde{\mathbf{g}}_{m-i}^*\mathbf{f}_0\right|^2\right]. \quad (40)$$

Now, we need to quantify each expectation on the right hand side (r.h.s.) of (40). Since $\tilde{\mathbf{g}}_{m-i}$ and $\mathbf{f}_0$ are independent and $\tilde{\mathbf{g}}_{m-i}$ is isotropically distributed in $\mathbb{C}^{M_t\times 1}$, the quantity $\left|\tilde{\mathbf{g}}_{m-i}^*\mathbf{f}_0\right|^2$ is beta distributed with parameter 1 and M_t-1 whose mean is given by $1/M_t$. Applying (6) with N_2 to the first term on the r.h.s. of (40) and using $\sum_{i=0}^{m-1}\epsilon^{2i} = (1-\epsilon^{2m})/(1-\epsilon^2)$ lead to

$$E\left[\left|\tilde{\mathbf{h}}_m^*\mathbf{f}_0\right|^2\right] = \epsilon^{2m}\left(1 - N_2\beta\left(\frac{M_t}{M_t-1}, N_2\right)\right) + \frac{1-\epsilon^{2m}}{M_t}.$$

This concludes that proof.

Appendix B
Proof of (8)

With the beta function equality $\beta(a,b) = \Gamma(a)\Gamma(b)/\Gamma(a+b)$, the quantity $N\beta\left(M_t/(M_t-1), N\right)$ can be equivalently rewritten by

$$\begin{aligned} &N\beta\left(\frac{M_t}{M_t-1}, N\right) \\ &= \frac{N\Gamma(N)\Gamma\left(\frac{M_t}{M_t-1}\right)}{\Gamma\left(N+\frac{M_t}{M_t-1}\right)} \\ &= \frac{N(N-1)\Gamma(N-1)\Gamma\left(\frac{M_t}{M_t-1}\right)}{\left(N+\frac{1}{M_t-1}\right)\Gamma\left(N-1+\frac{M_t}{M_t-1}\right)} \quad (41) \\ &= \left(\frac{N}{N+\frac{1}{M_t-1}}\right)(N-1)\beta\left(\frac{M_t}{M_t-1}, N-1\right). \quad (42) \end{aligned}$$

The equality in (41) follows from the fact $\Gamma(1+b) = b\Gamma(b)$. Note that (42) gives a recursion formula between quantization errors incurred by the codebook size N and codebook size $N-1$ Now, recursively applying (42) gives (8).

Appendix C
Proof of Theorem 1

Plugging (6) and (7) (in Lemma 1) into the average effective SNR loss in (5) gives

$$D_m^{\mathrm{snr}} = M_t\left(\epsilon^{2m}\left(\frac{M_t-1}{M_t}-\alpha_2\right) - \left(\frac{M_t-1}{M_t}-\alpha_1\right)\right). \quad (43)$$

The formula (43) indicates that D_m^{snr} is a monotonically decreasing function of m because $(M_t-1)/M_t = \beta\left(M_t/(M_t-1),1\right)$ and $\beta\left(M_t/(M_t-1),1\right) \geq \alpha_2$ due to (8). Thus, the optimization problem to find the maximum update period of the AFP scheme guaranteeing greater effective SNR gain than the MFP scheme is formulated by finding m such that[1]

$$m = \underset{\tilde{m}\ \mathrm{s.t.}\ D_{\tilde{m}}^{\mathrm{snr}}\geq 0}{\arg\min}\ D_{\tilde{m}}^{\mathrm{snr}}. \quad (44)$$

Then, the maximum feedback update period is $n = m+1$.

Manipulating (43) with the constraint $D_{\tilde{m}}^{\mathrm{snr}} \geq 0$ yields

$$\tilde{m} \leq \log_{\epsilon^2}\left(\frac{\frac{(M_t-1)}{M_t}-\alpha_1}{\frac{(M_t-1)}{M_t}-\alpha_2}\right). \quad (45)$$

Since $D_{\tilde{m}}^{\mathrm{snr}}$ is a monotonically decreasing function of $\tilde{m}$, the optimal m in (44) is the maximal positive integer satisfying (45), i.e.,

$$m = \left\lfloor \log_{\epsilon^2}\left(1 - \frac{\alpha_1-\alpha_2}{\frac{M_t-1}{M_t}-\alpha_2}\right)\right\rfloor_+ \quad (46)$$

where $\lfloor\cdot\rfloor_+$ denotes the flooring function to the nearest nonnegative integer. Since (46) is the achievable maximum channel index, this characterizes the bound on the feedback update period in (9). This concludes the proof.

Appendix D
Proof of Lemma 4

With the objective function $G_{B_2,\gamma}$, consider an optimization problem

$$B_{2,\mathrm{opt}} = \underset{\tilde{B}_2}{\arg\max}\, G_{\tilde{B}_2,\gamma}. \quad (47)$$

To solve this, we need to examine the behavior of $G_{\tilde{B}_2,\gamma}$. Differentiate $G_{\tilde{B}_2,\gamma}$ once with respect to $\tilde{B}_2$ yields

$$\begin{aligned} \frac{dG_{\tilde{B}_2,\gamma}}{d\tilde{B}_2} &= \epsilon^{2\left((\tilde{B}_2/\gamma)-1\right)}\left(\left(\frac{M_t-1}{M_t}\right)\ln\epsilon^{2/\gamma}\right. \\ &\left.+\Gamma\left(\frac{M_t}{M_t-1}\right)2^{-\tilde{B}_2/(M_t-1)}\left(\ln 2^{1/(M_t-1)} - \ln\epsilon^{2/\gamma}\right)\right). \quad (48) \end{aligned}$$

Equating $dG_{\tilde{B}_2,\gamma}/d\tilde{B}_2 = 0$ and after some algebraic manipulation, the equality $dG_{\tilde{B}_2,\gamma}/d\tilde{B}_2 = 0$ uniquely determines

$$\begin{aligned} \tilde{B}_2 &= (M_t-1) \\ &\times\log_2\left(\Gamma\left(1+\frac{M_t}{M_t-1}\right)\left(1+\gamma\frac{\ln 2^{-1/(M_t-1)}}{\ln\epsilon^2}\right)\right). \quad (49) \end{aligned}$$

We claim (49) is the maximizer of $G_{\tilde{B}_2,\gamma}$. In order to verify this, we first observe that $G_{0,\gamma} \leq 1/M_t$,

[1]One point to note is that the focus in (44) is on the largest feedback period such that infrequent high resolution feedback (the AFP scheme) outperforms frequent low resolution feedback (the MFP scheme). In this way, we can characterize the feedback update period n such that the AFP scheme yields larger a average effective SNR than the MFP scheme for every channel uses. It is possible to alternatively characterize the feedback update period n, using the average effective SNR averaged over all n channel uses. However, characterizing n with this averaged performance metric does not guarantee that the AFP scheme outperforms the MFP scheme for every channel uses.

$\lim_{\tilde{B}\longrightarrow\infty} G_{\tilde{B},\gamma} = 1/M_t$ and $G_{\tilde{B},\gamma} \geq 1/M_t$ for $\tilde{B} \geq \log_2(e)$ where the first inequality is due to the fact that $\gamma\left(M_t/(M_t-1)\right) \geq (M_t-1)/M_t$ in (19) and the last inequality comes from (16) and Lemma 4. Thus, if

$$\frac{dG_{\tilde{B},\gamma}}{d\tilde{B}}\Big|_{\tilde{B}=0} \geq 0 \tag{50}$$

the unique zero differential point in (49) is the maximizer. Otherwise, there is no single zero differential point. The condition in (50) can be readily seen by plugging $\tilde{B}_2 = 0$ in (48) and observing

$$\frac{dG_{\tilde{B}_2,\gamma}}{d\tilde{B}_2}\Big|_{\tilde{B}_2=0} = \epsilon^{-2}\left(\Gamma\left(\frac{M_t}{M_t-1}\right)\ln 2^{1/(M_t-1)} - \left(\Gamma\left(\frac{M_t}{M_t-1}\right) - \frac{M_t-1}{M_t}\right)\ln\epsilon^{2/\gamma}\right).$$

The facts $\ln\epsilon^{2/\gamma} < 0$ and $\Gamma\left(M_t/(M_t-1)\right) \geq (M_t-1)/M_t$ prove the claim. This concludes the proof.

Appendix E
Proof of Theorem 2

We first show the upper bound in (21). Note that with $B_{2,\mathrm{opt}}$ in (20), $G_{B_{2,\mathrm{opt}},\gamma}$ in (19) is always smaller than or equal to $F_{B_{2,\mathrm{opt}},\gamma}$ in (18). Thus, if $G_{B_{2,\mathrm{opt}},\gamma} \geq 1-\alpha_1, F_{B_{2,\mathrm{opt}},\gamma} \geq 1-\alpha_1$ is free. Equating $G_{B_{2,\mathrm{opt}},\gamma} \geq 1-\alpha_1$ gives

$$\epsilon^{2(B_{2,\mathrm{opt}}/\gamma-1)}\left(\frac{M_t-1}{M_t} - \Gamma\left(\frac{M_t}{M_t-1}\right)2^{-B_{2,\mathrm{opt}}/(M_t-1)}\right) \geq \frac{M_t-1}{M_t} - \alpha_1. \tag{51}$$

Factoring out $B_{2,\mathrm{opt}}$ from (51) to extract the bound on $B_{2,\mathrm{opt}}$ is not tractable. Other than directly solving (51), we use the first order condition found in Lemma 4. Equating $dG_{B_2,\gamma}/dB_2|_{B_2=B_{2,\mathrm{opt}}} = 0$ in (48) yields an equality

$$\epsilon^{2((B_{2,\mathrm{opt}}/\gamma)-1)}\left(\frac{M_t-1}{M_t} - \Gamma\left(\frac{M_t}{M_t-1}\right)2^{-(B_{2,\mathrm{opt}}/(M_t-1))}\right) = \frac{\left(\epsilon^{(2/\gamma)}2^{-(1/(M_t-1))}\right)^{B_{2,\mathrm{opt}}}\Gamma\left(\frac{M_t}{M_t-1}\right)\ln 2^{\gamma/(M_t-1)}}{-\epsilon^2\ln\epsilon^2}. \tag{52}$$

Plugging (52) in (51) and solving for $B_{2,\mathrm{opt}}$ gives the upper bound in (21). The lower bound follows from the fact that given $\gamma = B_{2,\mathrm{opt}}/n_{\mathrm{opt}}$, the condition $n_{\mathrm{opt}} \geq 1$ is equivalent to $\gamma \leq B_{2,\mathrm{opt}}$. This concludes the proof.

Appendix F
Proof of Theorem 3

From Theorem 1, the condition guaranteeing $n \geq \xi$ is equivalent to

$$1 - \frac{\alpha_1-\alpha_2}{\frac{M_t-1}{M_t}-\alpha_2} \leq \epsilon^{2(\xi-1)}. \tag{53}$$

Since we are interested in finding the minimum B_2 (i.e., $B_{2,\min}$) satisfying (53), the upper bound in (14) is applied to $\alpha_2 = 2^{B_2}\beta\left(M_t/(M_t-1), 2^{B_2}\right)$ in (53), which gives

$$\frac{1-\frac{M_t}{M_t-1}\alpha_1}{1-\frac{M_t}{M_t-1}\Gamma\left(\frac{M_t}{M_t-1}\right)2^{-B_2/(M_t-1)}} \leq \epsilon^{2(\xi-1)}. \tag{54}$$

After some algebraic manipulation, it is straight forward from (54) to show that the sufficient condition for $B_{2,\min}$ ensuring $n \geq \xi$ is obtained by

$$B_{2,\min} = \left\lceil (M_t-1)\log_2\left(\frac{-\Gamma\left(1+\frac{M_t}{M_t-1}\right)\epsilon^{2(\xi-1)}}{\left(1-\epsilon^{2(\xi-1)}\right)-\frac{M_t}{M_t-1}\alpha_1}\right)\right\rceil_+ \tag{55}$$

where $\lceil\cdot\rceil_+$ denotes the ceiling function to the nearest nonnegative integer. Note that the expression in (55) is only valid given

$$\left(1-\epsilon^{2(\xi-1)}\right) - \frac{M_t}{M_t-1}\alpha_1 \leq 0 \tag{56}$$

which is the condition that ensures the denominator inside of the $\log_2(\cdot)$ in (55) is negative. Accordingly, by applying the lower bound in (14) to α_1 in (56), a sufficient condition for the maximum B_1 denoted by $B_{1,\max}$ satisfying (56) is obtained by

$$B_{1,\max} = \left\lfloor (M_t-1)\log_2\left(\frac{1}{1-\epsilon^{2(\xi-1)}}\right)\right\rfloor_+. \tag{57}$$

This concludes the proof.

Appendix G
Proof of Lemma 5

We first check a convergence of

$$F_{X_B}(x) = \left(1-(1-x)^{aB-1}\right)^{2^B} \tag{58}$$

at a critical point. If $1-x$ in $F_{X_B}(x)$ is substituted by t, $F_{X_B}(x)$ can be rewritten in terms of t by $F_{T_B}(t) = \left(1-t^{-1}/t^{-aB}\right)^{2^B}$. By the definition of exponential function (i.e., $\lim_{i\longrightarrow\infty}(1-b/i)^i = e^{-b}$), when t is set as $t = 2^{-1/a}$, we have

$$\lim_{B\longrightarrow\infty} F_{T_B}\left(2^{-1/a}\right) = \lim_{B\longrightarrow\infty}\left(1-\frac{2^{1/a}}{2^B}\right)^{2^B} = e^{-2^{1/a}}. \tag{59}$$

Indeed, (59) implies $\lim_{B\longrightarrow\infty} F_{X_B}\left(1-2^{-1/a}\right) = e^{-2^{1/a}}$.

Now, the limiting behaviors of $F_{X_B}(x)$ when $x < 1-2^{-1/a}$ and $x > 1-2^{-1/a}$ as B tends to infinity are of interest. Dealing with a bound of the distribution function $F_{X_B}(x)$ provides tractable way to characterize $F_{X_\infty}(x)$ for $x < 1-2^{-1/a}$ and $x > 1-2^{-1/a}$.

Lemma 8: For $M_t \geq 1$ and $a = M_t/B$, the distribution function $F_{X_B}(x)$ in (58) is bounded by

$$e^{-2^B((1-x)^{aB-1})/(1-(1-x)^{aB-1})} \leq F_{X_B}(x) \leq e^{-2^B(1-x)^{aB-1}}. \tag{60}$$

Proof: For any real number $0 \leq y \leq 1$, natural logarithm inequality gives $-y/(1-y) \leq \ln(1-y) \leq -y$. Multiplying $N = 2^B$ to this inequality and rasing the base e of $\ln(1-y)$ gives

$$e^{-2^B y/(1-y)} \leq (1-y)^{2^B} \leq e^{-2^B y}. \tag{61}$$

If $aB \geq 1$ (or $M_t \geq 1$), the term $(1-x)^{aB-1}$ in (58) always lies in $[0,1]$. Thus, replacing y in (61) by $(1-x)^{aB-1}$ does not change the inequality in (61). ■

$x > 1-2^{-1/a}$: The convergence of $F_{X_B}(x)$ for $x = 1-2^{-1/a}+\eta$ with $0 < \eta \leq 2^{-1/a}$ as B, $M_t \longrightarrow \infty$ with fixed $a = M_t/B$, is evaluated by examining the lower bound $e^{-2^B((1-x)^{aB})/((1-x)-(1-x)^{aB})}$ in (60) at $x = 1-2^{-1/a}+\eta$

$$\begin{aligned}\lim_{B\longrightarrow\infty} & e^{-\left(2^{1/a}\left(2^{-(1/a)}-\eta\right)\right)^{aB}/\left(\left(2^{-(1/a)}-\eta\right)-\left(2^{-(1/a)}-\eta\right)^{aB}\right)} \\ &= \lim_{B\longrightarrow\infty} e^{-\left(1-\eta 2^{(1/a)}\right)^{aB}/\left(\left(2^{-(1/a)}-\eta\right)-\left(2^{-(1/a)}-\eta\right)^{aB}\right)} \\ &= 1 \end{aligned} \tag{62}$$

where (62) follows from the fact that $(1-\eta 2^{1/a}) < 1$ and $(2^{-1/a}-\eta) < 1$. Thus, the convergence in (62) implies

$$\lim_{B\longrightarrow\infty} F_{X_B}\left(1-2^{-1/a}+\eta\right) = 1.$$

$x < 1-2^{-(1/a)}$: In this case, we characterize convergence of $F_{X_B}(x)$ at $x = 1-2^{-1/a}-\nu$ with $0 < \nu \leq 1-2^{-1/a}$. Investigating the upper bound $e^{-2^B(1-x)^{aB-1}}$ in (60) at $x = 1-2^{-1/a}-\nu$ reveals

$$\lim_{B\longrightarrow\infty} e^{-\left(1+\nu 2^{1/a}\right)^{aB}/\left(\nu+2^{-1/a}\right)} = 0 \tag{63}$$

where (63) is due to $(1+\nu 2^{1/a}) > 1$. Thus, when $x < 1-2^{-1/a}$, the convergence in (63) implies

$$\lim_{B\longrightarrow\infty} F_{X_B}\left(1-2^{-1/a}-\nu\right) = 0.$$

Combining three convergence results for $x = 1-2^{-1/a}$, $x > 1-2^{-1/a}$, and $x < 1-2^{-1/a}$ leads to (33). This concludes the proof.

Appendix H
Proof of Lemma 6

To show (34), we first characterize quantities $\lim_{B,M_t\longrightarrow\infty} E[X_B]$ and $\lim_{B,M_t\longrightarrow\infty} E\left[X_B^2\right]$.

The first-order moment $E[X_B] = \int_0^1 x dF_{X_B}$ is broken into two integrals

$$\begin{aligned} E[X_B] &= \int_0^1 (1-F_{X_B}(x))\,dx \\ &= 1-\left(\int_0^{1-2^{-1/a}} F_{X_B}(x)dx + \int_{1-2^{-1/a}}^1 F_{X_B}(x)dx\right). \end{aligned} \tag{64}$$

Taking $\lim_{B\longrightarrow\infty}$ while maintaining $a = M_t/B$ to both sides of (64) gives

$$\begin{aligned} \lim_{B\longrightarrow\infty} & E[X_B] \\ &= 1-\lim_{B\longrightarrow\infty}\left(\int_0^{1-2^{-1/a}} F_{X_B}(x)dx+\int_{1-2^{-1/a}}^1 F_{X_B}(x)dx\right) \\ &= 1-\int_0^{1-2^{-1/a}} F_{X_\infty}(x)dx - \int_{1-2^{-1/a}}^1 F_{X_\infty}(x)dx \quad (65) \\ &= 1-\int_{1-2^{-1/a}}^1 1dx \quad (66) \\ &= 1-2^{-1/a} \quad (67) \end{aligned}$$

where the equality in (65) follows from the fact that since $F_{X_B}(x)$ is dominated by 1 (i.e., $F_{X_B}(x) \leq 1$) for all $B \geq 1$ and $F_{X_B}(x)$ converges to $F_{X_\infty}(x)$ (Lemma 5) for all $x \in [0,1]$, by using the dominated convergence theorem [27], changing the order of $\lim$ and $\int$ does not change the result. The equality in (66) is due to Lemma 5 and the fact that the value $F_{X_\infty}(x)$ at $x = 1-2^{-1/a}$ is negligible in computing $\int_{1-2^{-1/a}}^1 F_{X_\infty}(x)dx$, because the measure of a single discontinuity of $F_{X_\infty}(x)dx$ in $[0,1]$ is negligible.

Likewise, $E\left[X_B^2\right]$ is broken into two integrals as

$$\begin{aligned} E\left[X_B^2\right] &= \int_0^1 x^2 dF_{X_B} \\ &= 1-2\int_0^1 xF_{X_B}(x)dx \quad (68) \\ &= 1-2\left(\int_0^{1-2^{-1/a}} xF_{X_B}(x)dx+\int_{1-2^{-1/a}}^1 xF_{X_B}(x)dx\right) \quad (69) \end{aligned}$$

where (68) is obtained by integration by parts. Then, taking limits to both sides (69) gives

$$\begin{aligned} E\left[X_\infty^2\right] &= 1-2\left(\int_0^{1-2^{-1/a}} xF_{X_\infty}(x)dx+\int_{1-2^{-1/a}}^1 xF_{X_\infty}(x)dx\right) \\ &= 1-2\int_{1-2^{-1/a}}^1 xdx \\ &= \left(1-2^{-1/a}\right)^2. \end{aligned} \tag{70}$$

Consequently, from (67) and (70), as B, $M_t \longrightarrow \infty$ while $a = M_t/B$, the variance of X_B converges as

$$\lim_{B\longrightarrow\infty}\left(E\left[X_B^2\right]-E[X_B]^2\right) = 0.$$

This establishes $F_{X_B}(x) \longrightarrow F_{X_\infty}(x)$ in the mean-square sense, which implies $X_B \xrightarrow{\text{m.s.}} 1-2^{-1/a}$.

Appendix I
Proof of Lemma 7

First, an expression of $\lim_{M_t,B\longrightarrow\infty} |\tilde{\mathbf{h}}_m^*\mathbf{f}_0|^2$ is determined, and by using Lemma 6, the convergence result in (35) is verified.

Consider the effective SNR at $m = 1$.

$$\begin{aligned} |\mathbf{h}_1^*\mathbf{f}_0|^2 = \epsilon^2 |\mathbf{h}_0^*\mathbf{f}_0|^2 + (1-\epsilon^2)\,|\mathbf{g}_1^*\mathbf{f}_0|^2 \\ +2\epsilon\sqrt{1-\epsilon^2}\,\mathrm{Re}\left(\mathbf{f}_0^*\mathbf{h}_0\mathbf{g}_1^*\mathbf{f}_0\right) \end{aligned} \tag{71}$$

where $\mathrm{Re}(c)$ denotes a real part of $c \in \mathbb{C}$. Dividing (71) with $\|\mathbf{h}_1\|^2$ gives

$$\begin{aligned} \left|\tilde{\mathbf{h}}_1^*\mathbf{f}_0\right|^2 = \epsilon^2\frac{\|\mathbf{h}_0\|^2}{\|\mathbf{h}_1\|^2}\left|\tilde{\mathbf{h}}_0^*\mathbf{f}_0\right|^2 + (1-\epsilon^2)\,\frac{\|\mathbf{g}_1\|^2}{\|\mathbf{h}_1\|^2}\,|\tilde{\mathbf{g}}_1^*\mathbf{f}_0|^2 \\ +2\epsilon\sqrt{1-\epsilon^2}\,\frac{\|\mathbf{h}_0\|\,\|\mathbf{g}_1\|}{\|\mathbf{h}_1\|^2}\mathrm{Re}\left(\mathbf{f}_0^*\tilde{\mathbf{h}}_0\tilde{\mathbf{g}}_1^*\mathbf{f}_0\right). \end{aligned} \tag{72}$$

Now, we take B, $M_t \longrightarrow \infty$ to both sides of (72). The first term on the RHS of (72) is led to

$$\lim_{B,M_t\longrightarrow\infty}\frac{\|\mathbf{h}_0\|^2}{\|\mathbf{h}_1\|^2}\left|\tilde{\mathbf{h}}_0^*\mathbf{f}_0\right|^2 = \lim_{B,M_t\longrightarrow\infty}\left|\tilde{\mathbf{h}}_0^*\mathbf{f}_0\right|^2 \tag{73}$$

where $\lim_{M_t \to \infty} (\|\mathbf{h}_0\|^2/M_t)/\|\mathbf{h}_1\|^2/M_t = 1$, because $\|\mathbf{h}_0\|^2/M_t \to 1$ and $(\|\mathbf{h}_1\|^2/M_t) \to 1$ almost surely. Similarly, for the second term on the RHS of (72), taking B, $M_t \to \infty$ gives

$$\lim_{B,M_t \to \infty} \frac{\|\mathbf{g}_1\|^2}{\|\mathbf{h}_1\|^2} |\tilde{\mathbf{g}}_1^* \mathbf{f}_0|^2 = \lim_{M_t \to \infty} |\tilde{\mathbf{g}}_1^* \mathbf{f}_0|^2 \overset{\text{m.s.}}{=} 0 \quad (74)$$

where (74) follows from the fact that the quantity $|\tilde{\mathbf{g}}_1^* \mathbf{f}_0|^2$ is beta distributed with $\beta(1, M_t - 1)$ whose mean is $1/M_t$ and variance is $(M_t - 1)/(M_t^2(M_t + 1))$. Thus, as M_t goes infinity the mean and the variance converges to 0. This asserts $\lim_{M_t \to \infty} |\tilde{\mathbf{g}}_1^* \mathbf{f}_0|^2 \overset{\text{m.s.}}{=} 0$. For the third limit in (72), we have

$$\lim_{B,M_t \to \infty} \frac{\sqrt{\|\mathbf{h}_0\|^2 \|\mathbf{g}_1\|^2}}{\|\mathbf{h}_1\|^2} \mathrm{Re}\left(\mathbf{f}_0^* \tilde{\mathbf{h}}_0 \tilde{\mathbf{g}}_1^* \mathbf{f}_0\right) \overset{\text{m.s.}}{=} 0 \quad (75)$$

where (75) is due to the inequality $\mathrm{Re}\left(\mathbf{f}_0^* \tilde{\mathbf{h}}_0 \tilde{\mathbf{g}}_1^* \mathbf{f}_0\right) \leq \left|\mathbf{f}_0^* \tilde{\mathbf{h}}_0 \tilde{\mathbf{g}}_1^* \mathbf{f}_0\right| = \left|\tilde{\mathbf{h}}_0^* \mathbf{f}_0\right| |\tilde{\mathbf{g}}_1^* \mathbf{f}_0|$ and the fact that $\lim_{M_t \to \infty} |\tilde{\mathbf{g}}_1^* \mathbf{f}_0|^2 \overset{\text{m.s.}}{=} 0$. Combining (73), (74), and (75) yields

$$\lim_{B,M_t \to \infty} \left|\tilde{\mathbf{h}}_1^* \mathbf{f}_0\right|^2 \overset{\text{m.s.}}{=} \epsilon^2 \lim_{B,M_t \to \infty} \left|\tilde{\mathbf{h}}_0^* \mathbf{f}_0\right|^2. \quad (76)$$

Now, with the same procedure, for $m = 2$, we have

$$\left|\tilde{\mathbf{h}}_2^* \mathbf{f}_0\right|^2 = \epsilon^2 \frac{\|\mathbf{h}_1\|^2}{\|\mathbf{h}_2\|^2} \left|\tilde{\mathbf{h}}_1^* \mathbf{f}_0\right|^2 + \left(1 - \epsilon^2\right) \frac{\|\mathbf{g}_2\|^2}{\|\mathbf{h}_2\|^2} |\tilde{\mathbf{g}}_2^* \mathbf{f}_0|^2 + 2\epsilon\sqrt{1 - \epsilon^2} \frac{\|\mathbf{h}_1\| \|\mathbf{g}_2\|}{\|\mathbf{h}_2\|^2} \mathrm{Re}\left(\mathbf{f}_0^* \tilde{\mathbf{h}}_1 \tilde{\mathbf{g}}_2^* \mathbf{f}_0\right)$$

and taking $\lim_{B,M_t \to \infty}$ leads to

$$\lim_{B,M_t \to \infty} \left|\tilde{\mathbf{h}}_2^* \mathbf{f}_0\right|^2 \overset{\text{m.s.}}{=} \epsilon^2 \lim_{B,M_t \to \infty} \left|\tilde{\mathbf{h}}_1^* \mathbf{f}_0\right|^2 \overset{\text{m.s.}}{=} \epsilon^4 \lim_{B,M_t \to \infty} \left|\tilde{\mathbf{h}}_0^* \mathbf{f}_0\right|^2 \quad (77)$$

where (77) is due to (76). Now, it is straight forward for a general m,

$$\lim_{B,M_t \to \infty} \left|\tilde{\mathbf{h}}_m^* \mathbf{f}_0\right|^2 \overset{\text{m.s.}}{=} \epsilon^{2m} \lim_{B,M_t \to \infty} \left|\tilde{\mathbf{h}}_0^* \mathbf{f}_0\right|^2 \overset{\text{m.s.}}{=} \epsilon^{2m} \left(1 - 2^{-1/a}\right) \quad (78)$$

where (78) follows from Lemma 6. This concludes the proof.

Appendix J
Proof of Theorem 4

For the capacity loss in (26), the optimization problem finding $m_{\infty,\mathrm{cap}}$ is expressed as

$$m_{\infty,\mathrm{cap}} = \underset{\tilde{m} \text{ s.t. } D_{\tilde{m},\infty}^{\mathrm{cap}} \geq 0}{\arg\min} D_{\tilde{m},\infty}^{\mathrm{cap}}$$

where $D_{m,\infty}^{\mathrm{cap}}$ is given by

$$D_{m,\infty}^{\mathrm{cap}} = E\left[\lim_{B_1,B_2,M_t \to \infty} \log_2\left(\frac{1 + \rho \left|\mathbf{h}_m^* \mathbf{f}_0\right|^2}{1 + \rho \left|\mathbf{h}_m^* \mathbf{v}_m\right|^2}\right)\right].$$

Then, given $a_1 = M_t/B_1$ and $a_2 = M_t/B_2$, Lemma 6 and Lemma 7 leads to

$$\begin{aligned} D_{m,\infty}^{\mathrm{cap}} &= E\left[\lim_{B_1,B_2,M_t \to \infty} \log_2\left(1 + \frac{\rho \frac{\|\mathbf{h}_m\|^2}{M_t}\left(\left|\tilde{\mathbf{h}}_m^* \mathbf{f}_0\right|^2 - \left|\tilde{\mathbf{h}}_m^* \mathbf{v}_m\right|^2\right)}{\frac{1}{M_t} + \rho \frac{\|\mathbf{h}_m\|^2}{M_t} \left|\tilde{\mathbf{h}}_m^* \mathbf{v}_m\right|^2}\right)\right] \\ &= \log_2\left(1 + \frac{\epsilon^{2m}\left(1 - 2^{-1/a_2}\right) - \left(1 - 2^{-1/a_1}\right)}{\left(1 - 2^{-1/a_1}\right)}\right). \end{aligned}$$

Thus, $D_{m,\infty}^{\mathrm{cap}} \geq 0$ yields

$$\epsilon^{2m}\left(1 - 2^{-1/a_2}\right) - \left(1 - 2^{-1/a_1}\right) \geq 0. \quad (79)$$

Manipulating (79) gives the maximum available channel index $m_{\infty,\mathrm{cap}}$ as

$$m_{\infty,\mathrm{cap}} = \left\lfloor \log_{\epsilon^2}\left(\frac{1 - 2^{-1/a_1}}{1 - 2^{-1/a_2}}\right)\right\rfloor_+. \quad (80)$$

This gives the bound on the feedback update period $n_{\infty,\mathrm{cap}} \leq m_{\infty,\mathrm{cap}} + 1$ in (36).

For the effective SNR criterion, by taking B_1, B_2, $M_t \to \infty$ to (46), we can directly obtain

$$m_{\infty,\mathrm{snr}} = \left\lfloor \log_{\epsilon^2}\left(\frac{1 - 2^{-1/a_1}}{1 - 2^{-1/a_2}}\right)\right\rfloor_+ \quad (81)$$

which is equivalent to (80). This results in the same bound for $n_{\infty,\mathrm{cap}}$ and $n_{\infty,\mathrm{snr}}$. This concludes the proof.

References

[1] D. J. Love, R. W. Heath, Jr., V. K. N. Lau, D. Gesbert, B. D. Rao, and M. Andrews, "An overview of limited feedback wireless communication systems," *IEEE J. Sel. Areas Commun.*, vol. 26, no. 8, pp. 1341–1365, Oct. 2008.

[2] A. Narula, M. J. Lopez, M. D. Trott, and G. W. Wornell, "Efficient use of side information in mulitiple-antenna data transmission over fading channels," *IEEE J. Sel. Areas Commun.*, vol. 16, no. 8, pp. 1423–1436, Oct. 1998.

[3] K. K. Mukkavilli, A. Sabharwal, E. Erkip, and B. Aazhang, "On beamforming with finite rate feedback in multiple-antenna systems," *IEEE Trans. Inf. Theory*, vol. 49, no. 10, pp. 2562–2579, Oct. 2003.

[4] D. J. Love, R. W. Heath, Jr, and T. Strohmer, "Grassmannian beamforming for multiple-input multiple-output wireless systems," *IEEE Trans. Inf. Theory*, vol. 49, no. 10, pp. 2735–2747, Oct. 2003.

[5] J. C. Rho and B. D. Rao, "Transmit beamforming in multipl-antenna systems with finite rate feedback: A VQ-based approach," *IEEE Trans. Inf. Theory*, vol. 52, no. 3, pp. 1101–1112, Mar. 2006.

[6] P. Xia and G. B. Giannakis, "Design and analysis of transmit beamforming based on limited-rate feedback," *IEEE Trans. Signal Process.*, vol. 54, no. 5, pp. 1853–1863, May 2006.

[7] B. Banister and J. Zeidler, "Feedback assisted transmission subspace tracking for MIMO systems," *IEEE J. Sel. Areas Commun.*, vol. 21, no. 3, pp. 452–463, Apr. 2003.

[8] J. Yang and D. Williams, "Transmission subspace tracking for MIMO systems with low-rate feedback," *IEEE Trans. Commun.*, vol. 55, pp. 1629–1639, Aug. 2007.

[9] T. Inoue and R. W. Heath, "Geodesic prediction for limited feedback multiuser MIMO systems in temporally correlated channel," in *Proc. IEEE Radio and Wireless Syst.*, Jan. 2009, pp. 167–170.

[10] B. Mondal and R. W. Heath, "Channel adaptive quantization for limited feedback MIMO beamforming system," *IEEE Trans. Signal. Process.*, vol. 54, no. 12, pp. 4717–4729, Dec. 2006.

[11] R. Samanta and R. W. Heath, "Codebook adaptation for quantized MIMO beamforming systems," in *Proc. 39th Asilomar Conf.*, Oct. 2005, pp. 376–380.

[12] C. Simon and G. Leus, "Feedback quantization for linear precoded spatial multiplexing," in *EURASIP J. Adv. Signal Process.*, 2008, vol. 2008, p. 13.
[13] G. Leus and C. Simon, "Quantized feedback and feedback reduction for precoded spatial multiplexing MIMO systmes," in *Proc. Int. Symp. Signal Process. Its Appl. 2007 (ISSPA 2007)*, Feb. 2007.
[14] T. Kim, D. J. Love, B. Clerckx, and S. J. Kim, "Differential rotation feedback MIMO system for temporally correlated channel," in *Proc. IEEE Globecom*, Dec. 2008.
[15] K. Huang, R. W. Heath, and J. G. Andrew, "Limited feedback beamforming over temporally-correlated channels," *IEEE Trans. Signal Process.*, vol. 57, no. 5, pp. 1–18, May 2009.
[16] R. Chen, B. Hajek, and U. Madhow, "On fixed input distribution for noncoherent communication over high-SNR Rayleigh-fading channels," *IEEE Trans. Inf. Theory*, vol. 50, no. 12, pp. 3390–3396, Dec. 2004.
[17] R. H. Etkin and D. N. C. Tse, "Degree of freedom in some underspread MIMO fading channel," *IEEE Trans. Inf. Theory*, vol. 52, no. 4, pp. 1576–1608, Apr. 2006.
[18] C. K. Au-Yeung and D. J. Love, "On the performance of random vector quantization limited feedback beamforming in a MISO system," *IEEE Trans. Wireless Commun.*, vol. 6, no. 2, pp. 458–462, Feb. 2007.
[19] P. A. Dighe, R. K. Mallink, and S. S. Jamuar, "Analysis of transmit-receive diversity in Rayleigh fading," *IEEE Trans. Commun.*, vol. 51, pp. 694–703, Apr. 2003.
[20] M. K. Simon and M.-S. Alouini, *Digital Communications Over Fading Channels*. New York: Wiley, 2000.
[21] V. Raghavan, R. W. Heath, Jr., and A. M. Sayeed, "Systematic codebook designs for quantized beamforming in correlated MIMO channels," *IEEE J. Sel. Areas Commun.*, vol. 25, no. 7, pp. 1298–1310, Sep. 2007.
[22] J. G. Proakis, *Digital Communications*, 4th ed. New York: McGraw-Hill, 2000.
[23] L. L. Scharf, "Statistical signal processing: Detection," in *Estimation, and Time Series Analysis*. New York: Addison-Wesley, 1990.
[24] N. Jindal, "MIMO broadcast channels with finite-rate feedback," *IEEE Trans. Inf. Theory*, vol. 52, no. 11, pp. 5045–5060, Nov. 2006.
[25] W. Santipach and M. L. Honig, "Capacity of a multiple-antenn fading channel with a quantized precoding matrix," *IEEE Trans. Inf. Theory*, vol. 55, no. 3, pp. 1218–1234, Mar. 2009.
[26] IEEE 802.16m Evaluation Methodology Document (EMD) [Online]. Available: http://www.ieee802.org/16/tgm/index.html
[27] H. L. Royden, *Real Analysis*, 3rd ed. Englewood Cliffs, NJ: Prentice-Hall, 1988.

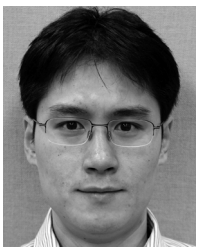

Taejoon Kim (S'08) received the B.S. degree (with highest honors) in electrical engineering from Sogang University, Seoul, Korea, in 2002, and the M.S. degree in electrical engineering from the Korea Advanced Institute of Science and Technology (KAIST), Daejeon, in 2004.

From 2004 to 2006, he was with the Electronics and Telecommunications Research Institute (ETRI), Daejeon. Since 2007, he has been pursuing the Ph.D. degree at Purdue University, West Lafayette, IN. He was a Summer Intern with the Samsung R&D Center, Richardson, TX, in 2008 and with the DSPS R&D Center, Texas Instrument, Dallas, in 2010, respectively.

David J. Love (S'98–M'05–SM'09) received the B.S. (with highest honors), M.S.E., and Ph.D. degrees in electrical engineering from the University of Texas at Austin, in 2000, 2002, and 2004, respectively.

Since August 2004, he has been with the School of Electrical and Computer Engineering, Purdue University, West Lafayette, IN, where he is now an Associate Professor. His research interests are in the design and analysis of communication systems, MIMO array processing, and array processing for medical imaging.

Dr. Love currently serves as an Associate Editor for the IEEE TRANSACTIONS ON SIGNAL PROCESSING and the IEEE TRANSACTIONS ON COMMUNICATIONS. He has also served as a Guest Editor for special issues of the IEEE JOURNAL ON SELECTED AREAS IN COMMUNICATIONS and the *EURASIP Journal on Wireless Communications and Networking*. He has been inducted into Tau Beta Pi and Eta Kappa Nu. Along with coauthors, he was awarded the 2009 IEEE TRANSACTIONS ON VEHICULAR TECHNOLOGY Jack Neubauer Memorial Award for the best systems paper published in the IEEE TRANSACTIONS ON VEHICULAR TECHNOLOGY in that year. He was the recipient of the Fall 2010 Purdue HKN Outstanding Teacher Award. In 2003, he was awarded the IEEE Vehicular Technology Society Daniel Noble Fellowship.

Bruno Clerckx (M'08) received the M.S. and Ph.D. degrees in applied science from the Universite Catholique de Louvain, Belgium.

He held Visiting Research Positions with Stanford University, Stanford, CA, and EURECOM Institute, France. He is currently with Samsung Advanced Institute of Technology, Samsung Electronics, Korea. He is the author or coauthor of one book on MIMO wireless communications and about 50 research papers. He has been actively contributing to 3GPP LTE/LTE-Advanced and IEEE 802.16m since 2007.